

**CLIPC DELIVERABLE (D -N°: 6.2)*****Observation-based CCII-T1s for the recent past and Performance metrics for climate model based CCII-T1s.****Dissemination level: PU (public)*Author(s): *Kari Luojus, Mikko Moisander, Jouni Pulliainen, Lars Barring, Renate Wilcke, Kristin Böttcher, Sari Metsämäki, Debbie Clifford, Yannis Bistinas, Christian Page, Milka Radojevic, Christiana Photiadou*Reviewer(s):
*Victoria Bennett, Luis Costa*Reporting period: *01/12/2013 – 30/11/2015*Release date for review: *17/06/2016*

Final date of issue:

Revision table			
Version	Date	Name	Comments
	7.3.2016		Internal review I
	23.5.2016		Internal review II
Final	17.6.2016		

Abstract

This document introduces observational datasets, both satellite- and reanalysis-based. Examples of CCII-T1's derived from these datasets and from climate model data are presented and possibilities for evaluation and bias correction of climate model data is discussed. There are historical datasets that can be used for this, but ground truth networks can be very sparse, with sampling done irregularly or with prohibitively large time steps in-between. This requires observations to be interpolated, and sometimes even extrapolated, both temporally and spatially and can cause great uncertainty in interpreting the results. Satellite-based and reanalysis datasets offer a new data source to compare against model based indicators that mostly gets around the interpolation problem. Both data sources however come with their own sources of uncertainty that users need to be aware of should they want to use these sources to verify results of their models. In this document are described activities from CLIPC task 6.2 to derivate observation based climate change indicators to be used in evaluation and bias correction of climate model based variables. Also first results from such evaluations are presented and implications they have on bias correction work is discussed.

Project co-funded by the European Commission's Seventh Framework Programme (FP7; 2007-2013) under the grant agreement n°607418

List of abbreviations

<u>CCII-T1s</u>	<u>Tier 1 Climate Change Impact Indicators</u>
<u>ESGF</u>	<u>Earth System Grid Federation</u>
<u>CCI</u>	<u>Climate Change Initiative program</u>
<u>ESA</u>	<u>European Space Agency</u>
<u>GCOS</u>	<u>Global Climate Observing System</u>
<u>UNFCCC</u>	<u>United Nations Framework Convention on Climate Change</u>
<u>ECVs</u>	<u>Essential Climate Variables</u>
<u>SWE</u>	<u>Snow Water Equivalent</u>
<u>DUE</u>	<u>Data User Element</u>
<u>SMMR</u>	<u>Scanning Multichannel Microwave Radiometer</u>
<u>SSM/I</u>	<u>Special Sensor Microwave Imager</u>
<u>SSMIS</u>	<u>Special Sensor Microwave Imager Sounder</u>
<u>ECMWF</u>	<u>European Center for Medium range Weather Forecasting</u>
<u>EASE-grid</u>	<u>Equal-Area Scalable Earth grid</u>
<u>SD</u>	<u>Snow Depth</u>
<u>HUT</u>	<u>Helsinki University of Technology</u>
<u>FSC</u>	<u>Fractional Snow Cover</u>
<u>SYKE</u>	<u>Finnish Environment Institute</u>
<u>SCA</u>	<u>Fraction of Snow Covered Area,</u>
<u>NASA</u>	<u>National Space Agency</u>
<u>MODIS</u>	<u>Moderate Resolution Imaging Spectroradiometer</u>
<u>NDSI</u>	<u>Normalized Difference Snow Index</u>
<u>CDR</u>	<u>Climate Data Record</u>
<u>SE</u>	<u>Snow Extend</u>
<u>ERS/ERS-2</u>	<u>two European Remote Sensing satellites, operated by ESA</u>
<u>ATSR-2</u>	<u>Along-Track Scanning Radiometer-2</u>
<u>AATSR</u>	<u>Advanced Along-Track Scanning Radiometer</u>
<u>NH</u>	<u>Northern Hemisphere</u>
<u>ECA&D</u>	<u>European Climate Assessment and Dataset</u>
<u>KNMI</u>	<u>The Royal Netherlands Meteorological Institute</u>
<u>WMO</u>	<u>World Meteorological Organization</u>
<u>RCC</u>	<u>Regional Climate Center</u>
<u>GFCS</u>	<u>Global Framework for Climate Services</u>
<u>ECA&D</u>	<u>The European Climate Assessment and Dataset</u>
<u>E-OBS</u>	<u>Gridded version of ECA&D</u>
<u>CRU</u>	<u>Climatic Research Unit</u>
<u>EU-FP6</u>	<u>Sixth Framework Programme European Union's Research and Innovation funding programme for 2002–2006</u>
<u>EU-FP7</u>	<u>Seventh Framework Programme European Union's Research and Innovation funding programme for 2007-2013.</u>
<u>EURO4M</u>	<u>The European Reanalysis and Observations for Monitoring</u>
<u>AVS</u>	<u>Annual Vegetation Stress</u>
<u>SeaWiFS</u>	<u>Sea-Viewing Wide Field-of-View Sensor</u>
<u>fAPAR</u>	<u>Absorbed Photosynthetically Active Radiation</u>
<u>JRC</u>	<u>Joint Research Center</u>

<u>SST</u>	<u>Sea Surface Temperature</u>
<u>AVHRR</u>	<u>Advanced Very High Resolution Radiometer</u>
<u>CEDA</u>	<u>Center for Environmental Data Archival</u>
<u>ATSR</u>	<u>Along Track Scanning Radiometer</u>
<u>DOY</u>	<u>Day of year</u>
<u>PCIC</u>	<u>Pacific Climate Impacts Consortium</u>
<u>ETCCDI</u>	<u>Expert Team on Climate Change Detection and Indices</u>
<u>WSDI</u>	<u>Warm Spell Duration Index</u>
<u>PIOMAS</u>	<u>Pan-Arctic Ice-Ocean Modelling and Assimilation System</u>
<u>ERA-CLIM</u>	<u>European Reanalysis of Global Climate Observations</u>
<u>RCM</u>	<u>Regional Climate Model</u>
<u>CORDEX</u>	<u>Coordinated Regional Climate Downscaling Experiment</u>
<u>RCA4</u>	<u>Rosby Centre regional atmospheric model</u>
<u>SMHI</u>	<u>The Swedish Meteorological and Hydrological Institute</u>
<u>DBS</u>	<u>Distribution Based Scaling</u>
<u>RPC45</u>	<u>Climate change scenario where emissions stabilize at 538 ppm by 2100</u>
<u>RCP85</u>	<u>Climate change scenario, where CO2 concentration will reach 936 ppm by 2100</u>
<u>CMIP5</u>	<u>Coupled Model Intercomparison Project, phase 5</u>
<u>SNW</u>	<u>Surface Snow Amount, CMIP5 variable</u>
<u>SNC</u>	<u>Surface_snow_area_fraction, CMIP5 variable</u>
<u>UKREAD</u>	<u>Reading University, UK</u>
<u>IDL</u>	<u>Interactive Data Language</u>
<u>NetCDF</u>	<u>Network Common Data Format</u>

Table of contents

Document structure.....	6
1 Objectives.....	6
2 Observation -based datasets relevant for CLIPC WP6	6
2.1 Relevant satellite-based datasets for CCII-T1s	6
2.1.1 Overview of ESA-CCI datasets	6
2.1.2 ESA GlobSnow Snow Water Equivalent (SWE)	8
2.1.3 CryoLand Fractional Snow Cover (FSC) data	10
2.1.4 ESA GlobSnow FSC data.....	11
2.2 Relevant reanalyses-based datasets for CCII-T1s	13
2.2.1 ECA&D	13
3 Derivation of climate change indicators from observation-based datasets	14
3.1 Derivation and examples of CCII-T1s from satellite data	14
3.1.1 ESA CCI datasets	14
3.1.2 Hemispherical Snow Mass	17
3.1.3 Derivation of snow melt dates from Satellite-based FSC observations (CryoLand/GlobSnow FSC)	18
3.1.4 Derivation of melting date using GlobSnow SWE data	19
3.2 Derivation and examples of CCII-T1s from reanalysis data.....	21
4 Utilization of observation-based data for bias correction	22
4.1 The use of remote sensing data for bias correction	22
4.2 Impact of bias correction of temperature and precipitation on CCII-T1s	24
5 Comparison and assessment of model-based and observation based CCII-T1s	25
5.1 Description of the model-based variables assessed and their comparability with satellite based observations.	25
5.2 Utilizing GlobSnow SWE data for assessing CMIP5 snow cover information	26
5.3 Comparison of satellite data with EURO-CORDEX Climate Model data	27
6 Summary and conclusions.....	32
References	33

Executive Summary

This report documents datasets published as deliverable 6.2 “Observation-based CCII-T1s for the recent past and performance metrics for climate model based CCII-T1s, where “CCII-T1” stands for “Tier 1 Climate Change Impact Indicators”. Three types of data are discussed: CCII-T1s calculated from observational data, CCII-T1s based on climate models, and observational and reanalysis data used for evaluation and/or bias-correction of model-based indicators.

A number of satellite based datasets for climate change indicator indices were acquired and assessed and results presented in this document. There are several promising candidates among, e.g. the ESA CCI programme, ESA GlobSnow and EC CryoLand that were documented and also examined for application for bias correction of climate model data.

In addition to describing produced datasets this document examines the challenges inherent in comparing model-based data to observational/reanalysis data and using these datasets for bias-correcting model based data. Both reanalysis- and satellite-based datasets have their own errors (due to modelling-, sensor characteristics and limitations) in turning the raw observations to variables that can be compared with those provided by climate models. While satellite-based observations have the advantage of providing large, usually global spatial coverage and providing data from remote locations where observations would otherwise be sparse or non-existent, they have their own set of challenges that need to be taken into account, such as data caps due cloud coverage and low light conditions or those caused by given instrument’s chosen orbit. This causes another source of uncertainty that needs to be taken into account when bias-correcting model-based data.

Additionally, the length of time-series is often a problem, as bias-correction needs to have several tens of years’ worth of data in order to take into account the natural variability; whereas suitable satellite time series are typically limited in time coverage to at most a few decades. The work carried out is a fair start for a field that has not been thoroughly investigated so far. Several problems and issues in the data and approaches suitable for the work were identified and early progress shows that there is potential to utilize the unique satellite-based datasets for both bias correction of climate model data and an independent “ground truth” reference data.

All the CCII-T1s will be available through the CLIPC portal. The climate model data will be available through the CLIPC portal and the Earth System Grid Federation (ESGF) web portal. Observational data is available through either ESGF or individual institutions responsible for producing said data.

Document structure

This is a documentation of work done as part of CLIPC WP6 and published as deliverable 6.2. Deliverable has six chapters. Chapter 1 gives us objectives of the document. Chapter 2 introduces us to observational datasets, both satellite- and reanalysis based, that have been used in calculating climate change indicators. Chapter 3 examines some indicators that are based on datasets introduced in previous chapter, explaining how they are produced and gives examples how they can be used. Chapter 4 examines the need to bias-correct outputs from climate models, and how satellite based observational data can be used for this purpose. Chapter 5 introduces us to two model based snow variables and examines how they compare with their observation based counterparts. Chapter 6 gives summary of work done and draws conclusions of lessons learned.

1 Objectives

The objective of this document is to give an introduction to observational datasets, both satellite- and reanalysis-based, to give examples of CCII-T1's derived from said datasets and compare how observational CCII-T1's agree with correspondent indices that are based on climate model data. The focus here is on snow variables and indices produced from these. Snow variables were chosen because of authors familiarity with them, because they have been used as input for Tier-2 indicators elsewhere in CLIPC project and because they are one of the few satellite based datasets that have uninterrupted time series of sufficient length available. Moreover, from a stakeholder perspective there is a strong need for climate scenarios for future snow condition, which is well established for winter tourism (e.g. Elsasser and Burki, 2002) and for biodiversity and population dynamics (e.g. Ovaskainen et al., 2013). At the same time, model evaluation of simulated snow conditions is difficult without high-quality spatially consistent and homogeneous observational datasets. Another goal is to examine the use of satellite-based observations as a benchmark for bias-correcting model-based data and give readers a reasonable understanding of the associated challenges.

2 Observation -based datasets relevant for CLIPC WP6

In this chapter we give introduction to a number of observation based datasets that have been used in CLIPC WP6 to calculate climate change indicators. In addition to description, a short history and directions how to access is given for each dataset.

2.1 Relevant satellite-based datasets for CCII-T1s

This section gives overview on observational datasets based on remote sensing, that have been used in CLIPC project. There is special focus on snow products due to their exceptionally long records that is 35 years of daily observations.

2.1.1 Overview of ESA-CCI datasets

This section provides an overview of the outputs from the Climate Change Initiative program (CCI) from the European Space Agency (ESA) and how they might be useful to derive climate impact indicators (CCII Tier-1).

The CCI program was initiated in response to the need for climate data that meet the guidelines and the requirements set by the Global Climate Observing System (GCOS) and the United Nations Framework Convention on Climate Change (UNFCCC). For more information on the GCOS guidelines see GCOS-195 (2015). Satellite datasets are now beginning to reach an appropriate length for climate studies, i.e.

a length of several decades. Depending on the variable in focus a record length of 20-30 years is often deemed necessary for forming climatological averages (and related statistics). However, for analysing climatological trends substantially longer time-series are normally needed. Essentially, the required record length, and averaging period, depends on the natural (internal) variability of the phenomenon analysed.

The main goal of the CCI program (see CCI portal: cci.esa.int) is to provide long-term climate datasets and their associated errors and uncertainties based on multi-sensor satellite archives. The project first conducted a user requirement analysis and includes documentation for the algorithm development and prototype “Essential Climate Variables” (ECV) building. The 13 ECVs chosen for the ESA-CCI are:

1. Aerosol Properties
2. Cloud properties
3. Fire Disturbance (Burnt area)
4. Greenhouse Gases (CO₂, CH₄)
5. Glaciers
6. Sea Ice
7. Ice sheets – Greenland
8. Ice sheets - Antarctica
9. Land Cover
10. Ocean Color
11. Ozone
12. Sea-level
13. Sea Surface Temperature
14. Soil Moisture

The Essential Climate Variables are derived from all available satellite data sources internationally and not just European (ESA). Moreover, each variable includes information about the errors and the uncertainties, but also information about the calibration, the validation and the algorithm used. The datasets are free to download (<ftp://anon-ftp.ceda.ac.uk/neodc/esacci/>, and through <http://cci.esa.int/data>). All variables are provided at global extent and at a variety of resolutions as appropriate for the variable and input data types. The temporal extent of the variables currently available is typically more than 10 years, except for the Cloud Properties data (2008-2009) and Fire Disturbance (2006-2008). The longest archive is that of Sea Ice that dates back to 1979. All the above-mentioned datasets are being extended in phase 2 of the CCI programme.

The CCI datasets provide an additional source of observation-based data for the derivation of climate impact indicators. The main advantage of using these satellite observations instead of in-situ observations is the broad geographical extent. Therefore, the ESA-CCI datasets are more suitable for studies at large scale (continental and global) and they cover areas where we cannot have in-situ measurements. However, one must account for retrieval uncertainties that can vary among different sensors and retrieval techniques, for inconsistencies in multi-sensor datasets, and that records for satellite based climate data are often much shorter than those from in-situ stations.

2.1.2 ESA GlobSnow Snow Water Equivalent (SWE)

The European Space Agency (ESA) Data User Element (DUE) GlobSnow project produced a hemispherical record of satellite-retrieved information on snow water equivalent (henceforth SWE). The SWE record on snow water equivalent was produced using a combination of passive microwave radiometer and ground-based weather station data, spanning years 1979 to 2014. The GlobSnow SWE retrieval utilizes a data-assimilation based approach combining space-borne passive radiometer data (SMMR, SSM/I and SSMIS) with data from ground-based synoptic weather stations. The satellite sensors utilized provide data at K- and Ka-bands (19 GHz and 37 GHz respectively) at a spatial resolution of approximately 25 km. The SWE record is produced on a daily, weekly and monthly basis. SWE information is provided for terrestrial non-mountainous regions of Northern Hemisphere, excluding glaciers and Greenland.

The SWE product has been generated using SWE retrieval methodology (Pulliainen 2006) complemented with a time-series melt-detection algorithm (Takala et al. 2009), full methodology described in detail in (Takala et al. 2011). The SWE retrieval and melt detection algorithms are combined to produce snow water equivalent maps incorporated with information on the extent of snow cover on coarse resolution (25 x 25km grid cells). The SWE estimates are complemented with uncertainty information on a grid cell level. The GlobSnow SWE processing system applies passive microwave observations and weather station observations collected by ECMWF in an assimilation scheme to produce maps of SWE estimates in EASE-grid (Equal-Area Scalable Earth grid, for details see Brodzik & Knowles, 2002) format over the northern hemisphere, covering all land surface areas with the exception of mountainous regions and Greenland. A semi-empirical snow emission model is used for interpreting the passive microwave (radiometer) observations through model inversion to the corresponding SWE estimates.

The basis of the SWE processing system is presented in an article by Pulliainen (2006). As applied for GlobSnow, estimates of SD (snow depth) based on emission model inversion of two frequencies, 18.7 and 36.5 GHz, are first calibrated over EASE grid cells with weather station measurements of available SD. Snow grain size is used in the model as a scalable model input parameter (being determined from the input radiometer and weather station data). These values of grain size are used to construct a Kriging interpolated background map of the effective grain size, including an estimate of the effective grain size error. The map is then used as an input in model inversion over the span of available radiometer observations, providing an estimate of SD. In the inversion process, the effective grain size in each grid cell is weighed with its respective error estimate. A snow density value is applied to each grid cell to connect depth to SWE. Areas of wet snow are masked according to observed brightness temperature values using an empirical equation, as model inversion of SD/SWE over areas of wet snow is not feasible due to the saturated brightness temperature response. The weather station observations of SD are further interpolated to provide a crude estimate of the SD (or SWE) background. The SWE estimate map and SD map from weather station observations are combined using a Bayesian spatial assimilation approach to provide the final SWE estimates.

The snow emission model applied is the semi-empirical HUT snow emission model (Pulliainen et al., 1999). The model calculates the brightness temperature from a single layer homogenous snowpack covering frozen ground in the frequency range of 11 to 94 GHz. Input parameters of the model include snowpack depth, density, effective grain size, snow volumetric moisture and temperature. Separate modules account for ground emission and the effect of vegetation and atmosphere. The model has been validated against tower-based and airborne reference radiometer observations (see e.g. Pulliainen et al., 1999, Lemmetyinen et al., 2009).

There are three separate SWE products, based on the same processing approach:

- **Daily Snow Water Equivalent** (Daily L3A SWE), snow water equivalent (mm) for each grid cell for all evaluated land areas of the Northern Hemisphere.
- **Weekly Aggregated Snow Water Equivalent** (Weekly L3B SWE), calculated for each day based on a 7-day sliding time window aggregation of the daily SWE product.
- **Monthly Aggregated Snow Water Equivalent** (Monthly L3B SWE), a single product for each calendar month, providing the average and maximum SWE, calculated from the weekly aggregated SWE product.

The weekly (7-day) aggregated product is calculated using sliding window averaging: the SWE estimate for the current day is calculated as a mean of the samples from the previous 6 days and the current day (for each grid cell). The monthly aggregate, a single product for each month, is calculated by determining the mean and the maximum of the weekly SWE samples. Examples of the daily and weekly SWE products are shown in Figures 2.1 and 2.2.; example of an uncertainty product is shown in Figure 2.3.

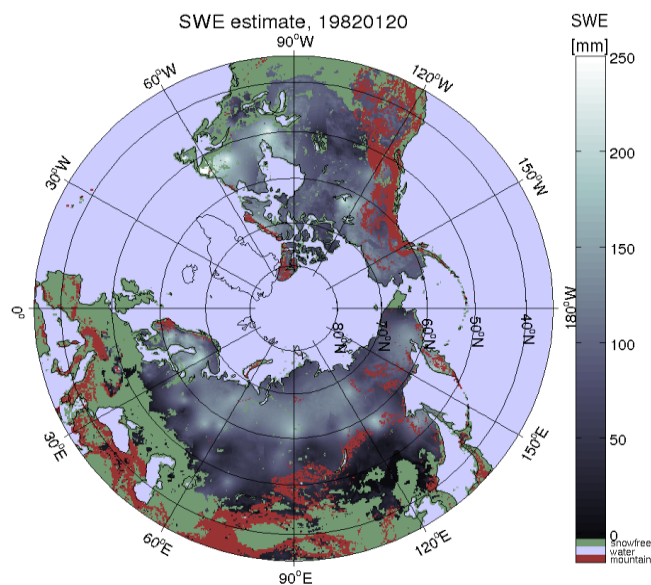


Figure 2.1: Example of a daily SWE product for 20 January 1982.

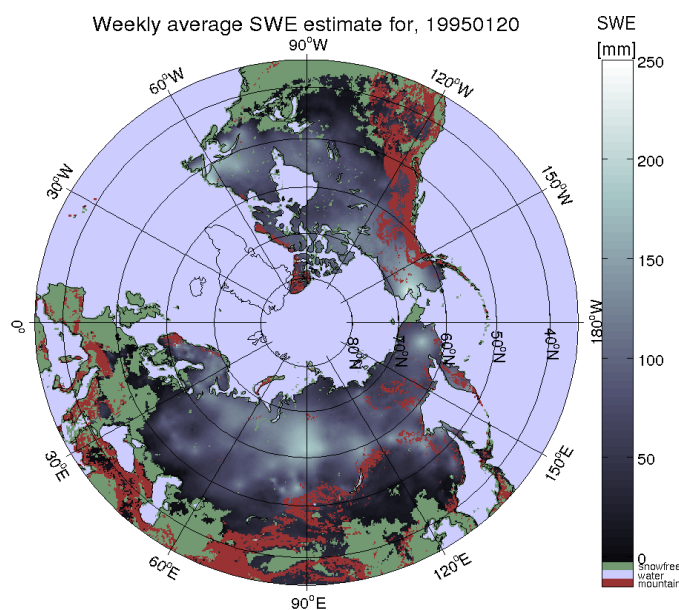


Figure 2.2: Example of a weekly aggregated SWE product for 20 January 1995.

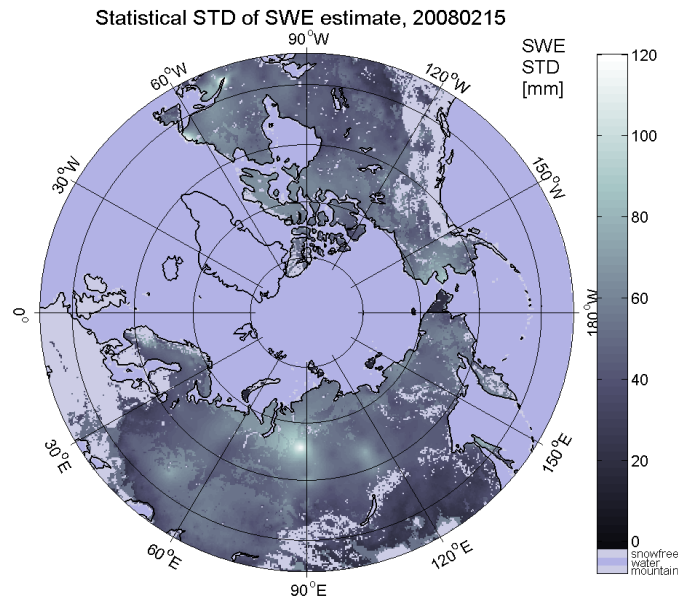


Figure 2.3: Statistical standard deviation of SWE estimate for 15 February 2008.

2.1.3 CryoLand Fractional Snow Cover (FSC) data

The CryoLand Pan-European snow cover service was established under EC-funded FP7-project “CryoLand- Copernicus Service Snow and Land Ice (2011-2015), coordinated by ENVEO IT GmbH (Innsbruck, Austria). SYKE provided a significant contribution to the regional Baltic Sea Area snow mapping service in its role as the algorithms developer and, correspondingly, to the development of the Pan-European scale snow cover mapping service (also based on the SYKE snow algorithm) utilized in CLIPC.

The CryoLand Pan-European snow cover service (Nagler et al., 2015) provides a homogeneous set of fractional snow cover products for years 2001-2014 for the area extending from 72°N/11°W to 35°N/45°E with a spatial resolution of 0.005° x 0.005° (corresponding roughly to 500m x 500m). FSC (Fractional Snow Coverage, or alternatively expressed, Fraction of Snow Covered Area, SCA) describes the percentage of snow-covered area for the total area of each grid cell. The product uses NASA Terra/MODIS reflectance data and official NASA MODIS cloud mask as input. The sub-pixel FSC retrieval relies on the radiative transfer theory-based SCAMod-reflectance model applied to the satellite reflectance observations at visible wavelengths (Metsämäki et al., 2005, 2012). The SCAMod-method was particularly designed to perform well also in forest areas, applying a pre-determined forest transmissivity map to account for the contribution of forests into the observed scene reflectance from the satellite footprint. The three major reflectance constituents (snow, snow-free ground and forest canopy) serve as model parameters. The essence of SCAMod is the forest canopy transmissivity, which has to be pre-determined for each product pixel. Basically, the transmissivity is produced by applying the SCAMod reflectance model for wintertime (full snow cover) satellite reflectance observations, and this was indeed done by SYKE for the production of CryoLand Baltic Sea area FSC-maps. However, in

order to generate a transmissivity values also for areas which very rarely (if ever) provide fully snow-covered conditions for the satellite sensor to observe, this basic methodology had to be complemented by Land Cover class-stratified statistical information on the transmissivities, gained through several data analyses in different parts of the target area. The methodology (which applies both for CryoLand and GlobSnow snow maps) is described in more detailed in Metsämäki et al., 2012 and 2015). Since SCAMod method is very sensitive to the reflectance fluctuations at the reflectance values close to those of a snow-free ground, an additional NDSI-thresholding is applied to discriminate between snow-free cases and snow cases: only those observations that pass the snow test are ingested by SCAMod otherwise FSC is set 0%. For CryoLand Pan-European FSC-production, this threshold is not fixed but is adjusted to change according to the latitude and altitude, so that in the south a higher NDSI is required to pass the snow test than in the north.

The CryoLand database is generated and maintained by ENVEO IT GmbH and data are freely available through the CryoLand GeoPortal (www.enveo.at). For the daily Pan-European FSC product also daily uncertainty giving the Root Mean Square Error per pixel is provided through the portal. The scientific support for the implementation of SCAMod and for establishing the service was provided by SYKE under the CryoLand-project. The Pan-European FSC dataset was extracted from there to SYKE for further analyses for the derivation of snow melt-off day information in CLIPC.

The uncertainty associated to FSC both in CryoLand and in GlobSnow SE products is an unbiased Root-Mean-Squared-Error based on the law of error propagation applied to the reflectance model used for FSC-estimation. This implies that the uncertainty does not include systematic error i.e. Bias is unknown. Since CryoLand and GlobSnow FSC use NDSI (Normalized Difference Snow Index) to identify snow-free areas (Metsämäki et al., 2012, 2015), it is actually NDSI that is the main driver for 'very low FSC' / 'snow-free' decision. According to (so far non-published) investigations there is a small negative bias at low snow fractions during the winter/spring period, and bias close to zero at full snow cover. For the accumulation period no investigation is done yet. However, since the FSC Bias is not yet fully investigated and particularly as it is not included in the uncertainty layer at the moment, it is recommended not to use the CryoLand uncertainty in bias correction of climate model data.

2.1.4 ESA GlobSnow FSC data

Besides SWE, the GlobSnow product portfolio includes maps of Fractional Snow Cover (FSC, range 0–100% or 0–1) on a $0.01^\circ \times 0.01^\circ$ (corresponding to 1 km x 1 km) geographical grid and they cover the Northern Hemisphere in latitudes 25°N – 84°N and longitudes 168°W – 192°E . GlobSnow SE products are based on optical and infrared data provided by ERS-2/ATSR-2 (1995–2003) and Envisat/AATSR (2002–2012), so that a continuous dataset spanning 17 years is obtained. Swath width for both ATSR-2/AATSR sensors is only ~500 km so complete spatial coverage at mid-latitudes cannot be achieved daily. Figure 2.4 presents the GlobSnow daily (Top), weekly aggregated (Middle) and monthly

aggregated (Bottom) snow extent maps. The difficulty caused by the narrow swath widths of the applied satellite sensors is evident, and regardless of the good thematic quality (as evaluated through in-situ validations), the data gaps limit the usability of SE data in certain applications, and particularly in those ones based on time series analysis at a pixel level.

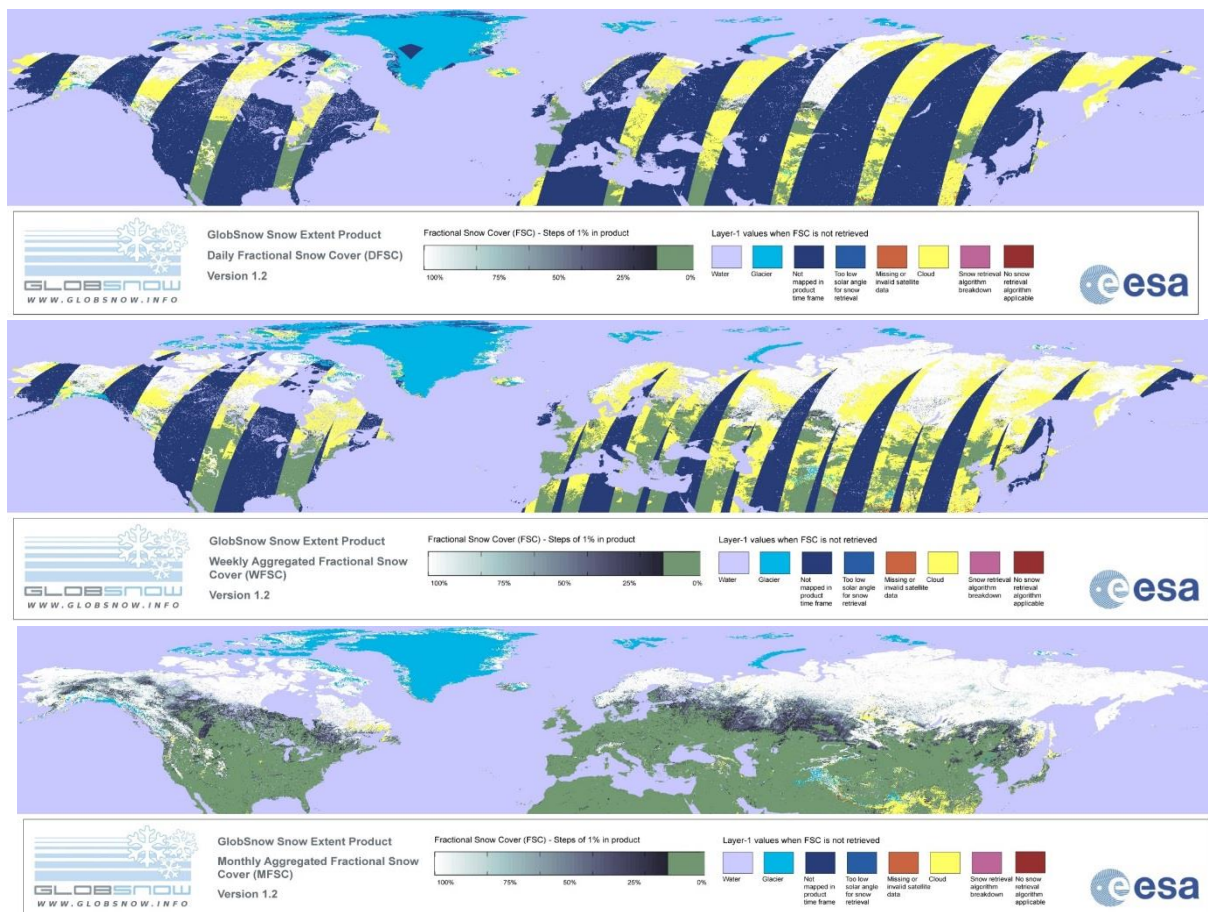


Figure 2.4. An example on a daily (Top), Weekly (Middle) and Monthly (Bottom) GlobSnow Snow Extent map.

The GlobSnow FSC relies on the SCAMod-reflectance model described above in Section 2.1.4. As discussed in 2.1.4, the determination of transmissivity map for almost whole of the Northern Hemisphere would not be possible based only on wintertime (from fully snow covered ground) satellite observations since there are extensive areas in NH which do not introduce a seasonal snow cover at all. Therefore, the transmissivity was generated (in the conventional SCAMod-based way) for seven training areas in different parts in NH, and then Global land Cover data (ESA GlobCover, Bicheron et al, 2009) and partly, also ESA GlobAlbedo data was employed to produce an estimate for a transmissivity based on statistical analyses between these datasets for each land pixel in the NH (see Metsämäki et al., 2015 for further details).

2.2 Relevant reanalyses-based datasets for CCII-T1s

This section introduces us to one reanalysis based dataset that can be used to calculate climate change indicators.

2.2.1 ECA&D

The European Climate Assessment and Dataset (ECA&D) is a joint effort of National Meteorological and Hydrological Services and other data holding institutions in Europe and the Mediterranean. It is operated by KNMI, and forms the backbone of the climate data node in the Regional Climate Center (RCC) for WMO Region VI (Europe and the Middle East) since 2010. The data and information products contribute to the Global Framework for Climate Services (GFCS). One of the products of ECA&D is the dataset E-OBS (currently v12.0, Haylock et al., 2008). E-OBS is a daily gridded observational dataset for precipitation, temperature (daily average, maximum, and minimum) and sea level pressure (van den Besselaar et al., 2011) in Europe. The current version of the full dataset covers the period 1950-01-01 until 2015-06-30 and monthly provisional updates are produced at the start of each new month. It was originally developed and updated as part of the ENSEMBLES (EU-FP6) and EURO4M (EU-FP7) projects. Currently, it is maintained, updated and elaborated as part of the UERRA project (EU-FP7). The E-OBS data are made available on a 0.25 ° and 0.5 ° regular lat–lon grid, as well as on a 0.22 ° and 0.44 ° rotated pole grid, with the North Pole at 39.25N, 162W. The regular grid is the same as the monthly CRU data grids available from the Climatic Research Unit. The rotated grid is the same as used in many ENSEMBLES Regional Climate Models. Besides 'best estimate' values, separate files are provided containing daily standard errors and elevation. The E-OBS data set is frequently used as a reference dataset for bias correction studies and projects, as it is one of the few surface-based observational gridded datasets with a daily resolution that is freely available, updated regularly and covering such a wide area of Europe.

3 Derivation of climate change indicators from observation-based datasets

This chapter introduces us to a number of observation based climate change indicators calculated from both satellite and reanalysis sources and used in CLIPC project.

3.1 Derivation and examples of CCII-T1s from satellite data

This section gives us examples of CCII-T1s calculated from satellite data sources introduced in chapter 2.

3.1.1 ESA CCI datasets

Derivation of CCII-T1s from satellite-based datasets

This section provides an overview of the use of satellite-derived data for climate impact indicators (CCII Tier-1) as specified in deliverable D7.1 ("A review of climate impact indicators across themes: Description of strengths, weaknesses, technical requirements and mismatches from expectations"; Costa et al, 2015). Additionally this section highlights some example cases for the use of remote sensing datasets in order to derive impact indicators.

Table 1 based on initial data gathering work done in D7.1 lists climate impact indicators (CCII Tier-1) that rely on satellite-derived products. The highlighted indicators belong to the subset of priority impact indicators. The input sensors and datasets in this table are based on the published methodologies of each indicator. There can be more than one dataset or variable involved for the building of the indicator. Other datasets not listed here, can also be used and some that were considered relevant and useful during this work will be described in the following sections.

No	Name of indicator	Datasets/sensors used
1	Arctic and Baltic Sea ice	Sea ice concentration from passive microwave brightness temperatures – SMMR (1979-1987) and SSM/I (1987-present)
4	Chlorophyll-a concentration	Surface reflectances - Envisat-MERIS (2003-2011), Aqua-MODIS (2012-2014)
23	Glaciers (observations/projections)	Snow extent (GlobSnow – optical measurements) – ERS-2 ATSR-2 (1995-2002) and Envisat AATSR (2002-2012)
25	Greenland ice sheet (observations)	Radar altimetry (ICESat, 2003-present), Gravimetry (GRACE, 2003-present), brightness temp. SMMR (1979-1987) and SSM/I (1987-present), MODIS (Global Land Cover, 2001).
31-32	Lake and river ice cover/phenology	Lake Ice Extent - CryoLand (optical measurements 2000-present) – Synthetic Aperture Radar (Envisat, RadarSAT, TerraSARX, Sentinel 1) (type, 1995-present)
33	Lake ice extent	Lake Ice Extent (CryoLand) - Synthetic Aperture Radar (Envisat, RadarSAT, TSX, S1, 1995-present)
43	Moth Phenology Index (observations)	Snow water equivalent (GlobSnow – passive microwave brightness temperatures 1979-present), Greening-up (NDWI), FAPAR start, maximum and end of season (MODIS 2001-present)
58	Sea level change	Radar altimetry – topex (1992-2001) and Jason missions (2001-present)
60	Sea Surface Temperature	AVHRR – Sea Surface Temperature (1982-2010)
62-63	Snow cover/extent	Snow extent (GlobSnow) – ERS-2 ATSR-2 (1995-2002) and Envisat AATSR (2002-2012)
64	SSPI: Standardized Snow Pack Index	Snow water equivalent (GlobSnow - passive microwave brightness temperatures) – SMMR (1979-1987), SSM/I and AMSR-E (1987-present)
81	Intensity of urban heat island with city size	MODIS land surface temperatures (2000-present), CORINE land cover (CLC2006)
85	Annual average damage from floods as fraction of GDP	CORINE land cover (CLC2006) – SPOT-4/5 and IRS P6 LISS III

Table 1. List of the Climate impact indicators from D7.1 (Costa et al 2015) that are derived from remote sensing data. The indicators refer to numbering (first column) used in deliverable D7.1 indicators. The highlighted indicators are priority indicators. The criteria used for the selection of the priority indicators follow the S.M.A.R.T. method (Doran 1981) as well additional criteria described in deliverable D7.1.

Remotely sensed data have strengths, but also show some limitations (Table 2). Remote sensing provides observations in broad geographical extent and is the only observational tool that can efficiently cover the whole globe. However, there remains a need for reliable in-situ data for validation.

Remote sensing platforms can be classified into active and passive sensors. Active sensors use their own power source to emit a signal to probe a target, typically relying on the backscattered signal for a measurement. Passive sensors measure naturally-emitted radiation or reflected sunlight to retrieve measurements. The majority of CCII's relate to surface variables, and the most relevant remotely sensed data exploit optical and microwave frequencies (see table 1, above).

Sensor/technique	Strengths	Limitations
Active (Radar)	Weather and daylight independent. Can penetrate clouds, light rain and snow. High resolution	Power consumption on board platform means historic missions often have limited sampling
Passive (Optical))	Long history of measurements leading to potential for longer datasets. Potential for high resolution measurements.	Requires sun illumination, therefore changes seasonally. Cannot penetrate the clouds. Tend to have limited swath, requiring many orbits for complete coverage.
Passive (Microwave)	Can see through clouds, unless precipitating heavily. Tend to have wide swath	Low resolution (25+ km pixels)

Table 2. Strengths and limitations of selected satellite remote sensing techniques.

The main limitation for indicators relying on data from optical and infrared sensors, like measurements for Chlorophyll concentration, Sea Surface Temperature, Snow Extent, Ice Extent and Land Cover, is the contamination of signal due to clouds. Therefore, there is always a challenge for consistency of the data concerning missing values and gap filling, but also using multiple sensors to cover the whole domain. For some variables, passive microwave data can be used, which can see through clouds that are not precipitating.

Examples of using remote sensing data to derive Climate Impact Indicators

Annual Vegetation Stress (AVS)

The vegetation stress indicator (McCormick & Gobron, 2015) attempts to give a measure of climate-related impact on vegetation. The principal reasons for such changes in vegetation are droughts, land use practices and changes in atmospheric CO₂ concentration. The core dataset used is 12 years of satellite data record (SeaWiFS and MODIS surface reflectances) of Absorbed Photosynthetically Active Radiation (fAPAR) that has been developed by the Joint Research Center (JRC) of the European commission. fAPAR is the fraction of solar radiation that is absorbed by the land vegetation during photosynthesis.

Vegetation stress is indicated by negative fAPAR anomalies (Figure 3.1). Annual fAPAR anomalies are computed and then aggregated at country level for 108 countries, taking into account the percentage of the pixels that show negative anomalies over the total vegetated area (Figure 3.2).

Analysis at country level show evidence of a good correspondence between large climatic phenomena and the values of vegetation stress index, as well as some lagged effect from previous year that becomes

obvious on next year's vegetation conditions. Auxiliary satellite datasets for this analysis are the forest extent data (LANDSAT data – Global Forest Cover Project) and the Global Land Cover (ESA-CCI).

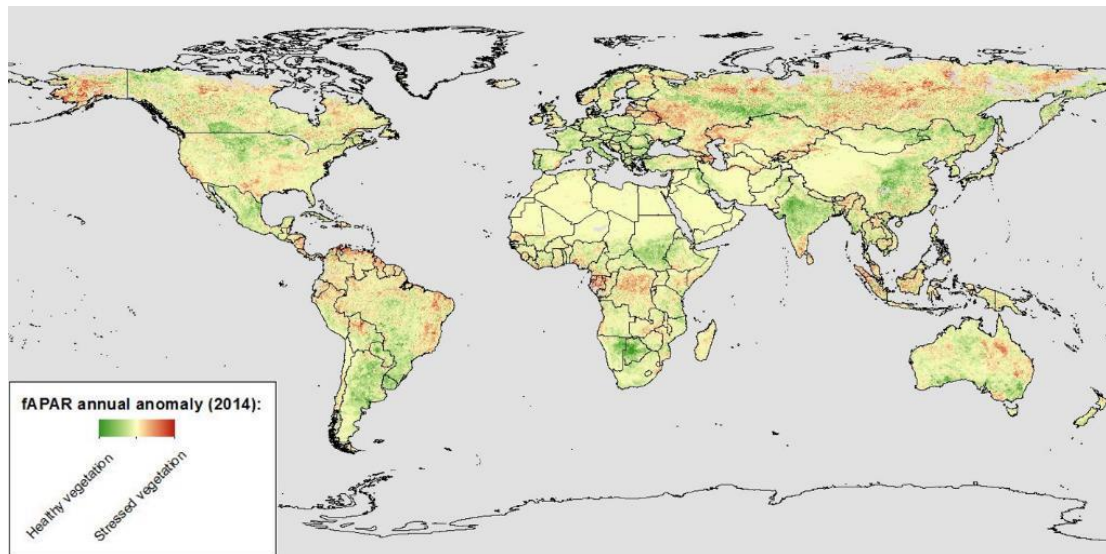


Figure 3.1. fAPAR anomalies for 2014. Negative anomalies are represented by red on the map.

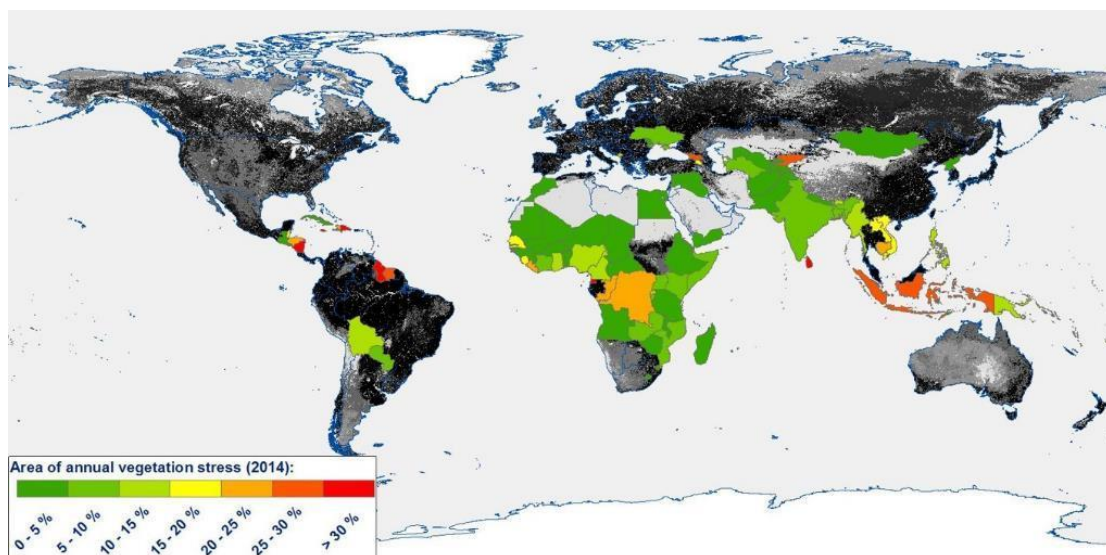


Figure 3.2. Percentage of pixels that show negative vegetation anomalies at country level.

This application provides a good example of how remote sensing is a valuable tool for monitoring vegetation at global scale and at country level, something impossible using in-situ measurements. Therefore, the indicator can be used for further analysis in combination to other global datasets and in global vegetation modelling.

Sea Surface Temperature (SST).

The SST impact indicator monitors the temperature changes of the ocean waters at global scale. Those changes are due to seasonal variations, ocean stream flow and climatic oscillations. Therefore the SST is by definition a climate impact indicator.

The impact indicator spreadsheet (part of D7.1) references the SST dataset exploiting optical (AVHRR) data from the NESDIS National Climatic Data Center (<http://www.ncdc.noaa.gov>). However, we would recommend the use of the SST product developed in the ESA CCI programme (Merchant et al 2014; data available through CEDA) as this is the first product specifically developed with climate requirements in mind. The CCI project combines time series from the Along Track Scanning Radiometer (ATSR) and the Advanced Very High Resolution Radiometer (AVHRR) sensors in order to derive a low-bias, climate-quality SST dataset. The main dataset includes daily time series of “skin” sea temperature at $\sim 10\mu\text{m}$ depth at morning (1030 am) and in the evening (2230 pm) starting from 1991 and extending to 2010. From this SST at 20cm depth is estimated after standardizing with respect to diurnal cycle. The main product (Level 4) covers the whole globe at 0.05° grid. The data are distributed with associated uncertainties, which makes it more robust and more reliable for use as an impact indicator. Monthly SST anomalies would be worth deriving as an alternative impact indicator calculated directly from daily SST data for the same period of the core dataset (Figure 3.3).

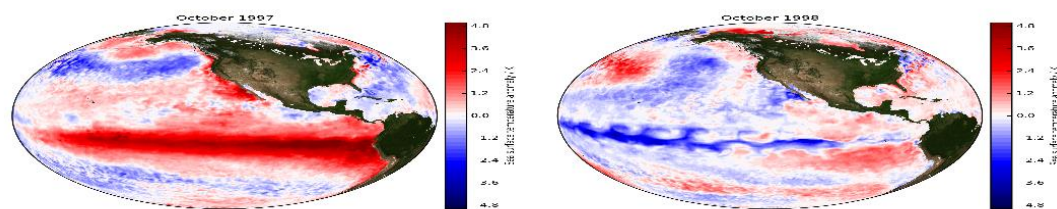


Figure 3.3. Monthly Sea Surface Temperature Anomalies for October 1997 and 1998 (<http://dx.doi.org/10.6084/m9.figshare.1189329>). In 1997 the development of the El Niño (El Niño Southern Oscillation) warm phase is clear and visible as a band of warm water in equatorial Pacific Ocean.

The SST anomalies are a suitable indicator for global scale studies and especially teleconnection studies. A monthly index for SST will show clearer the development of the El Niño phase and easier visualisation of year-to-year changes.

3.1.2 Hemispherical Snow Mass

The ESA GlobSnow SWE time series have been used to calculate an indicator of changes of the total terrestrial seasonal snow mass over the Northern Hemisphere. The daily SWE data have been used to calculate a monthly aggregate SWE representation for the Northern Hemisphere. This 25km resolution information is then used to calculate the total snow mass for the Northern Hemisphere for each month. The total snow mass values present the total average snow mass for the given month, when including all the terrestrial seasonal snow detected using the SWE retrieval approach. The total estimates do not include the snow/ice mass over glaciated regions, mountainous regions nor snow on ice sheets (i.e. on Greenland); the indicator does not estimate the snow on sea ice, but only the terrestrial snow. An example of a time series of Northern Hemisphere snow mass for the month of March, for the years 1980 to 2014 is presented in Figure 3.4.

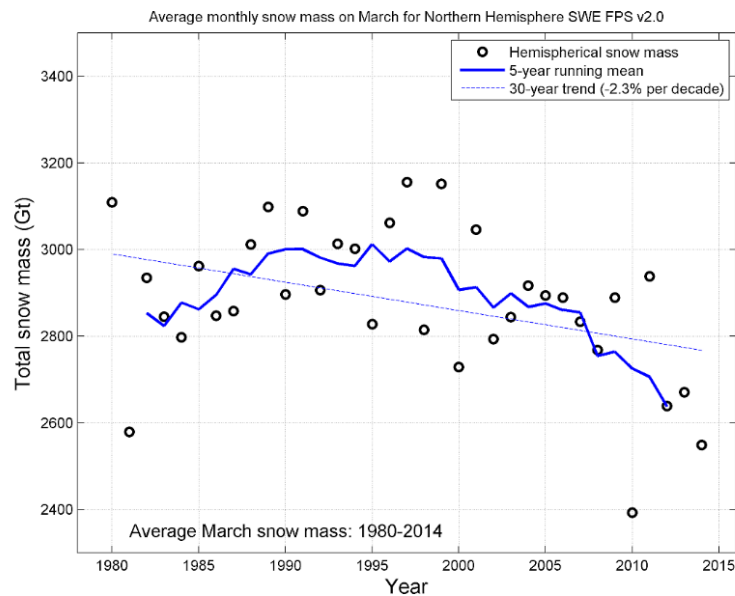


Figure 3.4: Time series of Northern Hemisphere snow mass for March, for the years 1980 to 2014.

Figure 3.4 provides an illustrative example of the strengths and weaknesses of a remote sensing dataset for climatological applications. The ESA GlobSnow SWE dataset provides a unique and valuable source for hemispherically integrated snow mass estimates over 35 years, which in the context of remotely sensed data is a very long period for a homogeneous dataset. However, for climatological studies the record is relatively short thus limiting its usability to analysing inter-annual variability as well as recent decadal variability, and not sufficient for establishing an independent source for long term trends.

3.1.3 Derivation of snow melt dates from Satellite-based FSC observations (CryoLand/GlobSnow FSC)

The melt-off day represents the best possible estimate for the day when the ground is completely snow-free and ends the snow season. This day is determined from Fractional Snow Cover (FSC) time series. Considering the fact that FSC-maps are produced from optical satellite imagery, the cloud obscuration poses a real problem to the accuracy of the melt-off day detection (as FSC can only be observed for clear-sky pixels). Considering this, having as many clear-sky FSC-observations as possible is crucial to the success of the melt-off day retrieval. This is why it was decided to use the Copernicus CryoLand FSC-time series as input to melt-off day retrieval instead of GlobSnow Snow Extent (also featuring FSC). The basic FSC-algorithm is the same for both these products (Metsämäki et al., 2005, 2012) but CryoLand – as relying on MODIS acquisitions with good spatial coverage – provide much more frequent observations than GlobSnow SE relying on ATSR-2/AATSR data suffering from large spatial gaps due to the sensor characteristics. The fact that GlobSnow provides longer time series would not justify its use for melt-off detection since in a worst case one may have only 1-2 clear-sky observations per month for a certain grid cell which is definitely too few considering the targeted accuracy of melt-off day detection (a few days).

When analysing the FSC time series evolving through the season, melt-off day is identified as a beginning of a at least few days' snow-free period (FSC=0%) after a period of snow observations (FSC > 0%). No temporal or spatial filtering is carried out. A snow period may include temporally sparse snow-free observations, whilst the snow-free period can include sporadic snow observations. This is necessary to allow, as the failure of cloud screening easily produces false snow commissions whereas undetected cloud shadows may produce false snow omission. However, a period of several snow occurrences after the already identified melt-off will launch a new snow period and a new melt-off day will be determined as a follower to that one. For deciding on the start of a new snow period or a new snow-free period, the required minimum number of snow observations (or snow-free observations, respectively) is applied. This number cannot be determined as a fixed number due to the typically frequent cloud-obscured observations; instead the number is based on the ratio of clear-sky observations to the total number of observations within a few days' period. Figure 3.5 present examples on the derived melt-off day maps generated from CryoLand data (years 2007 and 2010 shown here, out of the total number of 14 maps for year 2001-2014) demonstrating how the timing of the snow melt can be very different in different years.

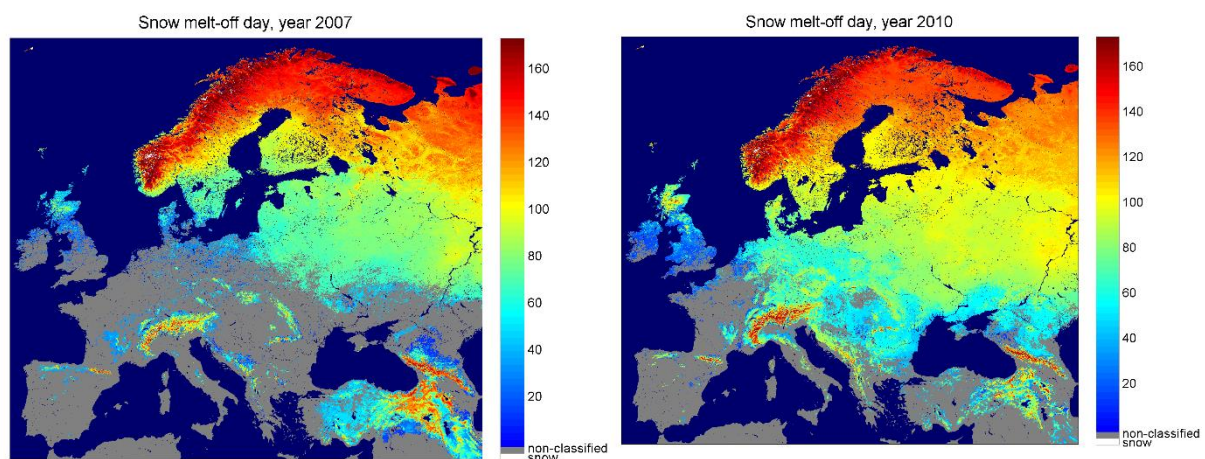


Figure 3.5. Snow Melt-off maps for year 2007 (left) and for 2010 (Right), as derived from CryoLand Pan-European Fractional Snow Cover (FSC) products. Day is given as Day of Year, i.e. starting from January the 1st in each year. Grey colour indicates areas for which the melt-off day was not possible to determine (intermittent snow or no snow days at all)

3.1.4 Derivation of melting date using GlobSnow SWE data

In addition to the SWE information, the GlobSnow SWE products include information on the overall extent of snow cover. The information on snow extent can be derived from SWE by utilizing the following coding for the SWE product, whereby SWE values of:

- 0 mm denotes snow-free areas (assumed Snow Extent 0%)
- 0.001 mm denote areas with melting snow (Snow Extent undefined between 0% and 100%; no SWE retrieval because of the wet state of the snow cover)
- > 0.001 mm denote areas with full snow cover (assumed Snow Extent 100%)

The areas that have been flagged as snow-free or melted are identified using a time-series melt detection approach described in Takala et al. (2009). The areas that are identified as wet snow or have no SWE retrieval, but are identified as snow covered with the time-series melt-detection approach, are denoted with a SWE value of 0.001 mm. The areas that are determined as snow-free or melted by the melt-detection approach, are denoted with a SWE value of 0 mm. All the other areas show a retrieved SWE value (that is in all cases greater than 0.001 mm).

The detection of snow melt-off (snow clearance) day is based on a time-series melt detection approach described in (Takala et al. 2009). The algorithm can be used to determine the end of snow-melt season using the available radiometer observations on a hemispherical scale covering the GlobSnow SWE time-series up to present day. The methodology has been calibrated against a vast Pan-Arctic dataset covering most of the land-areas of Northern Eurasia between the years 1979 to 2001. Product time series cover the years from 1979 to present day. Figure 3.6 presents how start day of the melting season has changed from 1980 to 2007.

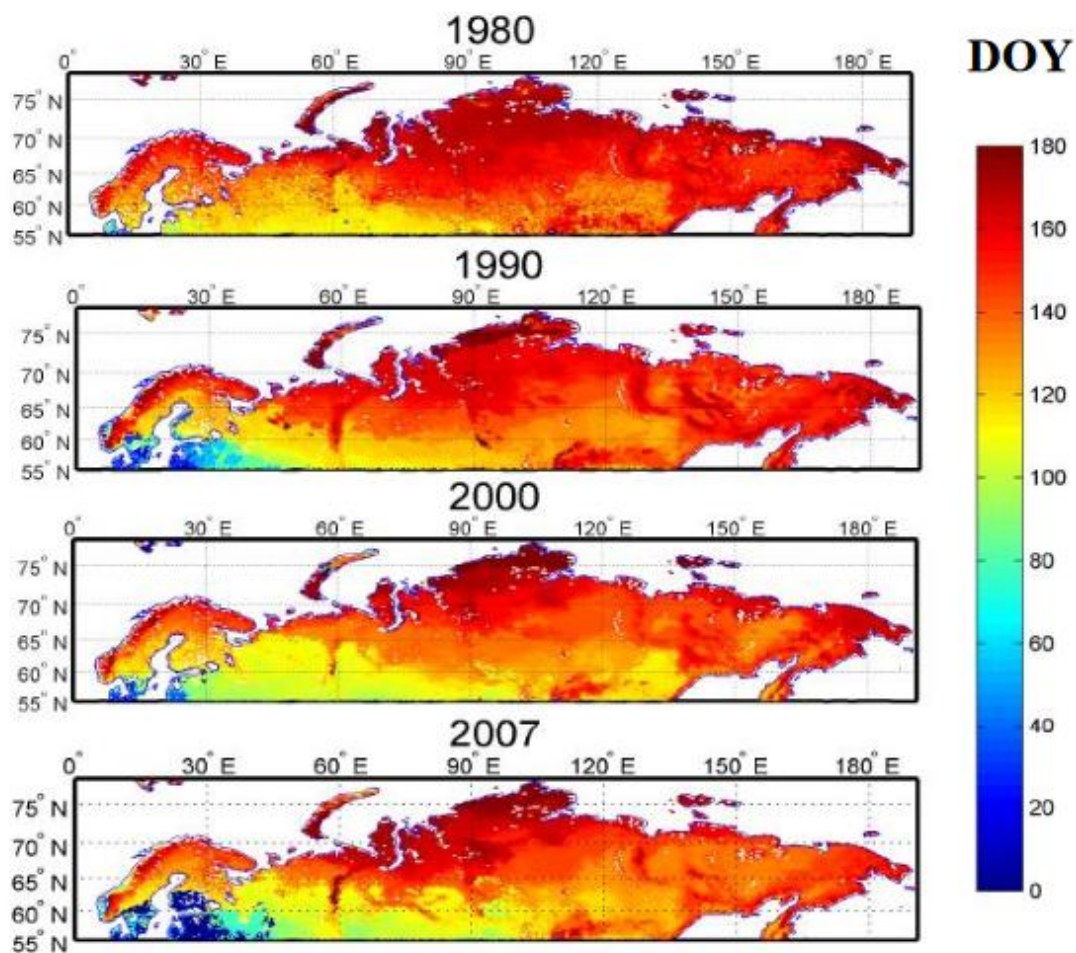


Figure 3.6: Evolution of melt-off (snow clearance) date from 1980 to 2007 using time-series approach. The colour code is the number of days since January 1 each year. The scale is capped to 180 days, so maximum value means 180 days or later.

3.2 Derivation and examples of CCII-T1s from reanalysis data

KNMI worked on the derivation of CCII-T1s from the E-OBS data set. All calculations of the CCII-T1s are done with the R package `climdex.pcic.ncdf` (and the backbone `climdex.pcic`) developed by the Pacific Climate Impacts Consortium (PCIC). This R library contains the code to calculate all the 27 calculations for the ETCCDI indices (CCI/CLIVAR/JCOMM Expert Team on Climate Change Detection and Indices, Klein Tank et al., 2009), on which the CCII-T1s are based. KNMI is working also in close collaboration with the PCIC to adapt the `climdex.pcic` library with a set of indices which are not part of the ETCCDI set but already available from the ECA&D webpages. ECA&D makes use of two advantages of these R libraries in updating the gridded CCII-T1s; one is the use of the bootstrapping routine proposed by Zhang et al., (2005), which avoids inhomogeneity in percentile-based indicators of temperature extremes; second, the libraries incorporate parallel computation which reduces the calculation time of the indicators. KNMI also prepared a specific E-OBS indices maps page and data portal where users of ECA&D can view, download and interact with the mapping of the indices and time series (Fig 3.7). A future development of the page will be the incorporation of uncertainties for each indicator. This is still work in progress which is reflected in the calculation of the WSDI indicator (Warm Spell Duration Index). This index is currently calculated without the bootstrapping approach where in a newer version of the library it will be included. Future changes in the R library are the incorporation of new frequencies for some indices (monthly, seasonal, half-year) and the addition of an additional set of indices. This part is done in close collaboration with the EUPORIAS (EU-FP7) project.

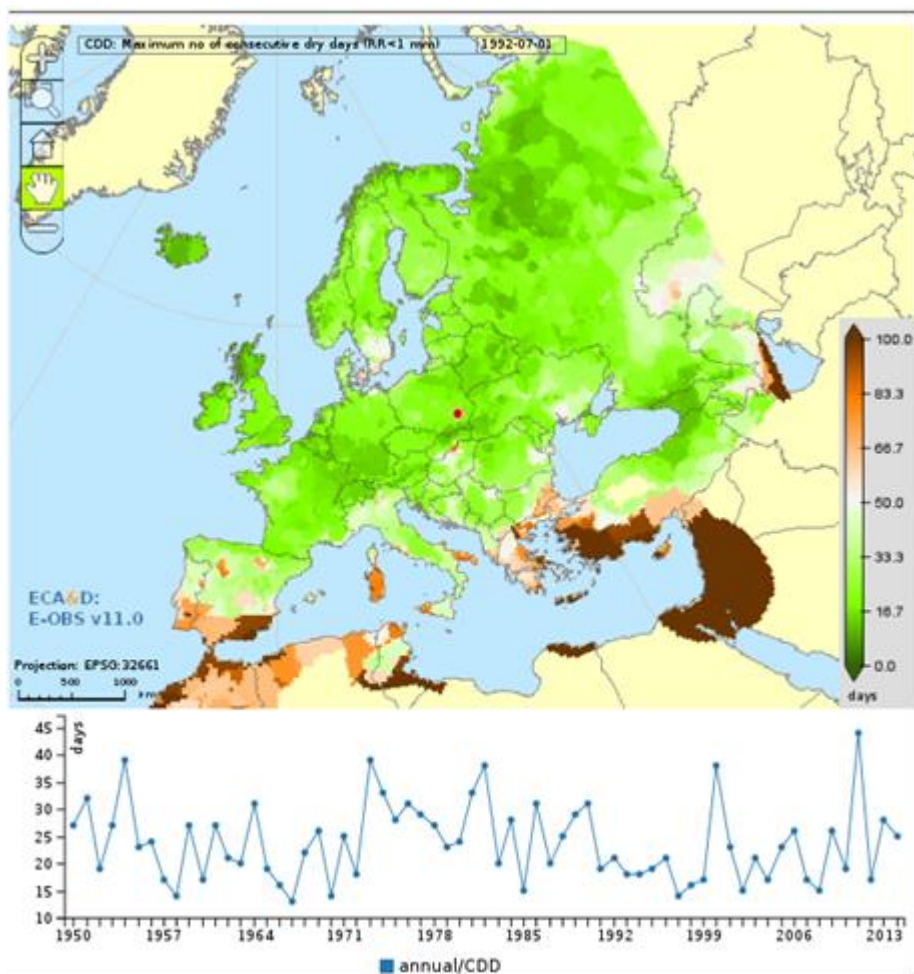


Figure 3.7: Example of the E-OBS indices page showing the CDD (Consecutive Dry Days) for 1992, with the viewing processes of the CCII-T1s and the eca indices. Clicking on the map provides a time series of the index for the selected frequency.

As an example, Fig. 3.8 shows the percentile-based index of warm days (TX90p) for the summer (Jun-Jul-Aug) of 2014, using 1981-2010 as base period. This summer was somewhat disappointing in terms of warm days for Central and South Europe, while for northern Scandinavia the number of warm days was much higher than usual.

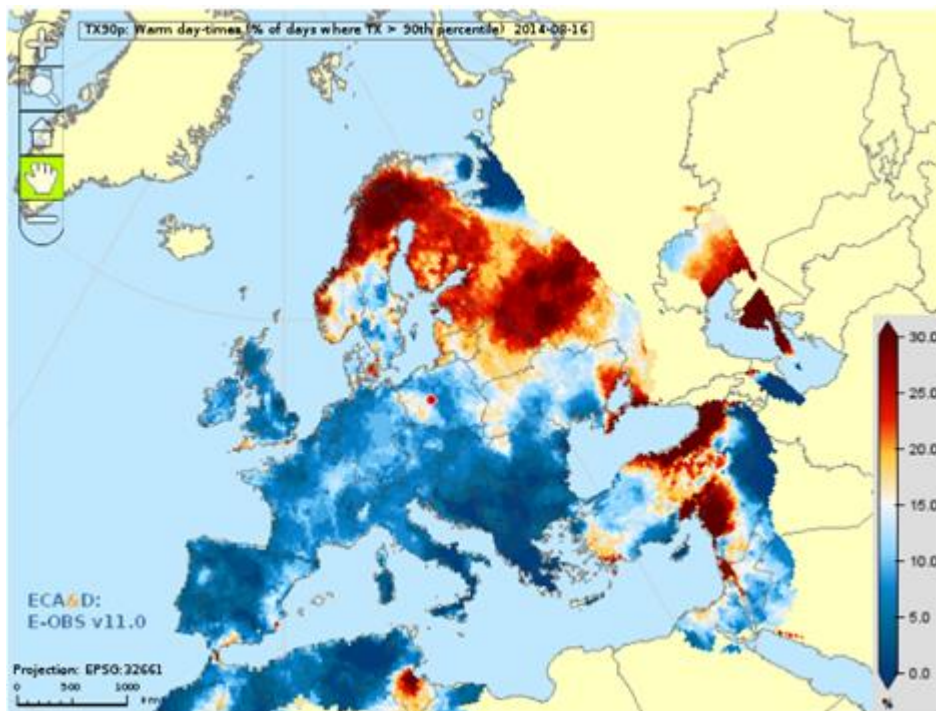


Figure 3.8: Warm days in % for summer (June-July-August) 2014

4 Utilization of observation-based data for bias correction

4.1 The use of remote sensing data for bias correction

The need for Bias Correction of Climate data

General Circulation Models are an essential tool for looking at future climate and looking at past variability. These model outputs include biases. Biases are the component of errors that are constant in time, and bias correction is the elimination of these systematic errors. Such biases include systematic model errors caused by conceptualization of the physical structure of the model and spatio-temporal discretization. Typical biases lead to the incorrect estimation of extremes and incorrect seasonal variations. Therefore, a bias adjustment of climate model outputs is essential before their use by the impacts modelling community (e.g. Christensen et al., 2008 and Seneviratne et al., 2012). This section examines the advantages and limitations of using remote sensing data for bias correction.

A basic bias correction procedure adjusts the mean of a time series by adding the averaged differences between model outputs and a set of reference observations, or by applying a correction factor to the differences. Further adjustment might be achieved by correcting the difference between the variance of the simulated and the variance of the observed parameter and other moments like skewness.

Inter-comparison of Bias correction methods shows that each method has different strengths and weaknesses, and the most appropriate method depends on the characteristics of the variable, type of benchmarking data used and their statistical properties (see e.g. Themeßl et al., 2011 and Watanabe et al., 2012). Nonetheless, bias adjustments inevitably introduce an additional level of uncertainty. The CLIPC project is making use of particular techniques for bias correction, based on "quantile mapping" (see Wilcke et. al., 2015 for details).

Satellite data as a benchmark for Bias Correction

Remote sensing offers the possibility of performing bias correction over a broad geographical extent; whereas in situ data consist of measurements at a point that typically do not provide a regular grid. Additionally, satellite data provide measurements where is inaccessible for in-situ measurements due to rough terrain and no access in remote areas. Bias correction methods require long time series in order to be able to provide robust statistics to support the bias correction procedure. The available literature doesn't provide a desirable length for reference data, although in the majority of the studies this is more than two decades. Existing studies predominantly use in situ observations, but there is now potential to exploit long time series of climate data from satellites that cover a broad geographical extent. However this involves stitching together measurements over time from multiple instruments, which can increase uncertainties and make biases hard to assess. The majority of satellite products do not exceed 15 years of observations, which is considered relatively short for a robust bias correction. The ESA DUE GlobSnow SWE data (see Takala et al., 2011) from the Finish Meteorological Institute is exceptionally long. The product provides 35 years of data. However, deriving variables like the "end-date of the snow season" (a variable required for input into certain climate impact indicators) reduces the time series to annual data points and therefore to 35 values (for each pixel); in these cases, longer time series (e.g. from in situ sensors) may be more appropriate.

Finally, there are large differences in resolution of observations and model outputs. That would mostly influence bias correction of regional model outputs that need high-resolution products. The upcoming ESA's Sentinel missions will provide six satellite constellations that consist of two satellites each in order to provide better coverage and promising high resolution down to 10 meters. The new missions are expected to strengthen the role of remote sensing data for bias correction although the short time series remains the basic limitation. Our literature review has found no published examples of the use of remote sensing data for bias correcting climate model outputs in the available literature (Web of science, Google scholar). We are aware of one recent study (Melia et al., 2015) that uses satellite and in situ data assimilated into the Pan-Arctic Ice-Ocean Modelling and Assimilation System (PIOMAS) to correct estimates of the date of an ice-free Arctic in models. CLIPC may become the first project to publish bias correction using remotely sensed data directly.

In order to overcome the problem of short data records, an alternative would be to use reanalysis data. Global reanalysis data prevail in terms of temporal extent over both in-situ and satellite observations. Reanalysis products use data assimilation techniques in order to assimilate observations and model simulations in order to provide a record that can extent back in time. The European Reanalysis of Global Climate Observations (ERA-CLIM) is the first product to be developed for use in climate studies (ERA-CLIM; www.era-clim.eu). As always, these datasets also need careful assessment of their biases before they can be used for bias correction. Both the data assimilation schemes and the observing system vary over time, which can cause discontinuities and apparent trends in the end dataset.

Summary

In summary, remote sensing data offer a promising reference for bias correction of climate data, whose potential has not yet been tested or exploited in the literature. The main advantage is the broad geographical extent essential for continental and global climate studies. Problems using remote sensing data as benchmark arise due to the short time series (compared to in situ data) and, for the longest datasets, the complexity in understanding biases in products that are constructed from multiple instruments. Recent climate-oriented reanalysis datasets also provide a promising source of reference data, but again the biases need to be carefully assessed.

4.2 Impact of bias correction of temperature and precipitation on CCII-T1s

A high-resolution, regional climate change information also takes into account the climate indices as derived from daily time series of 2m air temperatures and precipitation. The CCII-Tier1 indicators are referred here to as a subset (Costa et al., 2015) of the ETCCDI (Ccl/WCRP/JCOMM Expert Team on Climate Change Detection and Indices) core climate indices. The CCII-Tier1s therefore include the extremes over a specific period as well as the day-count based indices (number of days over a given/specific threshold). A generic open-source *Python* package (*icclim*: <https://github.com/cerfacsglobc/icclim>), is the software tool for generating the CCII-Tier1s within the CLIP-C.

In impact studies, the Regional Climate Model (RCM) output are often required to be bias corrected (Christinsen et al., 2008). However, the effect of a statistical bias correction (hereafter, BC) among other factors depends on the nature of atmospheric field (temperature or precipitation) and its regional characteristics within the climate system. We thus investigate whether the BC of 2m temperatures and precipitation improves a reliability of the CCII-Tier1s within European continent. Moreover, the focus is over relatively large regions, non-uniform in terms of topography and climate variability.

To identify the key features of the CCI-Tier1s that are sensitive to the bias adjustment, the CCII-Tier1s were generated from a high-resolution RCM output, without and with bias correction. The perceptual comparison of statistical similarity metrics over land is based on the long-term average and corresponding variance (year-to-year variability). The reference baseline climate is represented by the EUR-11 EURO4M-MESAN re-analysis (Bärring et al., 2014).

Preliminary climate change dataset of bias-corrected 2m air temperature and precipitation from the CORDEX RCA4 experiment, produced at SMHI has been made available within CLIPC (Milestone M25). Both historical run and the future projection (following RPC45 and RCP85 scenarios) cover the EUR-11 CORDEX domain, with a spatial resolution of 0.11 degree of latitude and longitude. The corresponding bias adjustment technique is Distribution Based Scaling (DBS) with the EUR-05 EURO4M MESAN (1989-2010) regional reanalysis as a reference data set (see Wilcke et al., 2015).

The initial comparison over land indicate an overall increase in spatial uniformity of the CCII-Tier1s in the regions with high altitude such as Alps and Scandinavian mountains when using the BC input data. However, the regions with a higher annual variability of the CCII-Tier1s (central and eastern Europe), the BC based data shown a decrease in confidence comparing to the reference reanalysis data. The level of associated uncertainties for each CCII-Tier1 varies across selected frequency (months, seasons). Since the BC has been performed independently on temperature and precipitation, the index performance varies among the CCII-Tiers1.

To obtain more generic assessment of the effects of BC input on the CCII-Tiers1s at European level, a spatial clustering of the indicators should be performed. This implies construction of a composite index for the reference climate and in second phases for the future projections.

5 Comparison and assessment of model-based and observation based CCII-T1s

This chapter gives us an example of two climate model based snow variables, compares them with their observation based counterparts and examines factors affecting such comparisons

5.1 Description of the model-based variables assessed and their comparability with satellite based observations.

This section describes climate model-based snow variables and examines factors affecting comparison with satellite-based observations.

CMIP5 (Coupled Model Intercomparison Project, phase 5) is a project that aims to evaluate how realistic climate models are in simulating recent past and to understand some of the factors responsible for differences between different model projections through a set of standard tests. CMIP5 also provides projections of future climate change on two time scales, near term (out to about 2035) and long term (out to 2100 and beyond).

One of key tools in making sure different models and also outside data sources can be successfully compared is a careful and formalized definition of terms and variables used.

In CMIP5 variable list each variable is given official name, abbreviation, measured unit and long name. Additionally a short description might follow.

Following model-based variables from CMIP5 were compared against corresponding satellite-based data:

Surface Snow AmountSNW kg m-2

Computed as the mass of surface snow on the land portion of the grid cell divided by the land area in the grid cell; reported as 0.0 where the land fraction is 0; excluded is snow on vegetation canopy or on sea ice.

Corresponding satellite-based dataset GlobSnow SWE, this variable was compared against, has seas and other major water areas masked out. There are however smaller subpixel sized water bodies with snow on ice, that will influence the amount of snow detected. On global scale, like in comparison detailed in 5.2 the difference is small, but on local scale and in coastal areas this can affect comparison of GlobSnow dataset and models following CMIP5 definition of SNW variable.

Snow Area Fraction % snc surface_snow_area_fraction

Percentage of a pixel that is snow covered.

Both CryoLand and GlobSnow FSC datasets used in this project are based on optical satellite data and suffer from data gaps caused by clouds and/or sensor coverage. Also polar night means that greater part of Northern latitudes can't be observed at all. Uneven spatial and temporal coverage caused by these factors limit comparability of SNC variable to regional test areas where data is more consistently available. Details of one such comparison can be found in 5.3.

5.2 Utilizing GlobSnow SWE data for assessing CMIP5 snow cover information

An assessment of climate model simulations from the CMIP5 archive on SNW is carried out using the GlobSnow SWE dataset. The objective of this work was to investigate the performance of the CMIP5 models in capturing the evolution of hemispheric scale snow conditions for the period of 1980 to 2014. The climate model simulations on snow water equivalent (CMIP5 model parameter “SNW”) are evaluated against the GlobSnow SWE record. The future projections of the CMIP5 model simulations on snow cover are also investigated.

The results indicate a clear decreasing trend in spring time hemispherical snow mass for the period of 1980 to 2014 in remote-sensing based data record. The inter-comparison of satellite-based record and climate model simulations show large differences in autumn, winter and spring time Hemispherical scale snow conditions. Trends of decreasing snow cover are also seen in the investigated CMIP5 models, although there is a notable variance between different models. Some of the models capture the overall hemispherical snow mass more accurately than others. In general the winter months (December, January and February) seem to be rather well captured, while the spring season, (March, April and May) appears more challenging for the climate models. Also the inter-annual variability of snow cover is higher in the observation-based record, compared with climate models.

The evaluation of the total snow mass over northern hemisphere was carried out for a large number of CMIP5 models and compared with the satellite-based data record. The evaluated CMIP5 data were sample into the 25x25km EASE grid, used for GlobSnow SWE, and were masked in similar manner to GlobSnow SWE data. Thus the SWE data over Greenland, glaciers, and mountainous regions of Northern Hemisphere were masked out (removed) from the CMIP5 dataset; as the SWE estimation using satellite data for those regions is extremely challenging. However, the evaluated data set includes regions that are mostly affected by seasonal snow. Therefore, this study describes the change we are observing in the seasonal snow pack. The preliminary analyses have been conducted using a subset of all available data; including models, all of which contain historical data and data acquired using RCP85 emission scenarios for future.

The conducted evaluations show that the CMIP5 ensemble average is rather close to the satellite-based data record for the overlapping time period during the winter months on January and February as seen in Figure 5.1. For March the CMIP5 ensemble average is significantly higher than that of the satellite-based record as seen in Figure 5.2. For April, the CMIP5 ensemble average shows a significant over estimation when compared with the satellite-based data, as shown in Figure 5.2. This indicates that the satellite-based and CMIP5 based data are agreeing relatively well regarding the overall hemispherical

snow mass for the winter months, but the CMIP5 models are not as accurate in catching the hemispheric snow mass during the spring snow melt season.

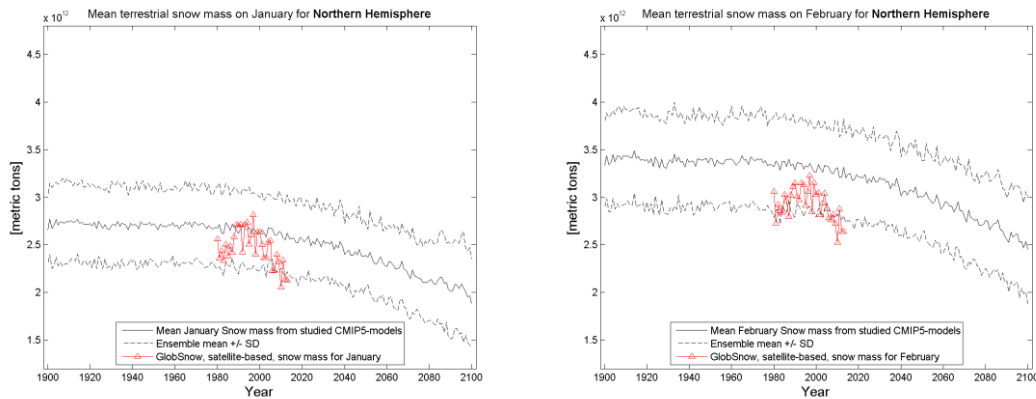


Figure 5.1: CMIP5 ensemble from 16 investigated models, compared with GlobSnow satellite-based SWE record for Northern Hemisphere for **January and February**. CMIP5 record includes historical simulations extended to future using RCP85 emission scenarios. Left hand figure presents January, right hand figure presents February.

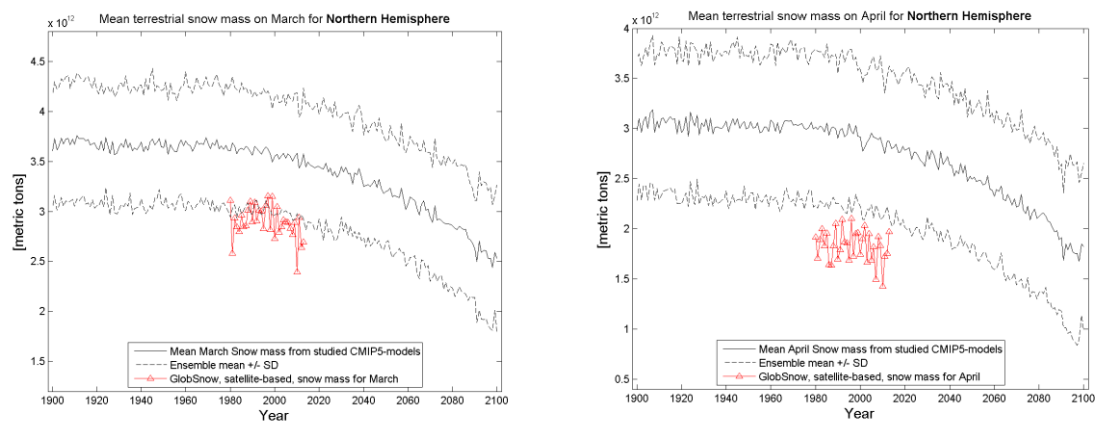


Figure 5.2: CMIP5 ensemble from 16 investigated models, compared with GlobSnow satellite-based SWE record for Northern Hemisphere for **March and April**. CMIP5 record includes historical simulations extended to future using RCP85 emission scenarios. Left hand figure presents March, right hand figure presents April.

5.3 Comparison of satellite data with EURO-CORDEX Climate Model data

From the outset of the work package it was agreed to try to apply bias correction (quantile mapping) on snow data products derived from satellites. At a workshop held at SMHI, researchers from FMI, SYKE, UKREAD, and SMHI met to learn about snow data from satellites, snow from regional climate models, as well as how to apply bias correction on climate models.

During the workshop we learned that the GlobSnow Snow Water Equivalent (SWE) product has weaknesses in coastal and mountain areas as well as during the melt-off season. On the other hand, we

identified a scaling error in the data packing and output module of the regional modelling system SMHI-RCA4 rendering the SWE data unusable. As a result, it was not possible to make progress on further analyses of SWE as long as the Earth System Grid Federation (ESGF) services are not available to allow access to SWE data from other regional climate models.

As an alternative, the CryoLand Fractional Snow Cover (FSC) product is available. It has an improved spatial coverage, due to applying a wide swath sensor and is more robust in some areas where GlobSnow SWE shows weaknesses. And fractional snow cover is a readily available output variable from SMHI-RCA4. The SMHI-RCA4 SWE error pertained only to the output module and not the internal process modelling related to snow, meaning that the model output FSC is not affected.

Therefore, we decided to focus on CryoLand FSC to explore the applicability for bias correction, not least because the start and end of the snow cover season is an important factor for many applications related to climate impacts on natural and managed environments. This document describes the initial analyses of FSC and the prospects to harmonising the SMHI-RCA4 FSC and CryoLand daily_FSC_PanEuropean_Optical datasets with respect to spatial and temporal resolution, as well as “consistency of information content”.

Data – technical details

The dataset which has been used is provided by the CryoLand project (<http://cryoland.enveo.at/>). CryoLand offers fractional snow cover (FSC) for the Pan-European region on daily temporal resolution and at 500m × 500m horizontal resolution.

As this is a rather huge dataset with mostly no snow cover, we decided to focus on a few selected study regions. Initially, we have cut out a sub-region (Figure 5.3) in southern Sweden, with the coordinates:

Min longitude	Max longitude	Min latitude	Max latitude
13.132873	15.960610	56.244196	57.291434

Those files can be downloaded with an IDL script (`scripting_wcs_analyse_v1.1.pro`) provided on the web-page of CryoLand project. Within the script one can easily define sub regions and periods to download. We started the download of a test region in Southern Sweden. The reasoning was to analyse a region with as much snow cover as possible, but also with as much data as possible. Regions further north are shadowed during winter and therefore do not provide satellite data. However, from a practical perspective the restriction of 99 files for each download process, turned out to be a limiting factor that complicated the download.

The files contain daily data for each 500m × 500m grid cell with values representing the actual FSC or, alternatively missing value code, different types of error codes relating to clouds or otherwise circumstances other than snow.

With kind assistance from the organisation, ENVEO IT GmbH, Innsbruck, that is hosting the data server we received the whole Pan-European data set for the period November 2001 to 2015 formatted as daily GeoTiff formatted files (1.3 Tb). The request for the whole data set is related to the thought of providing data in the Clip-C portal, but also to be flexible during the analysis process, to choose additional sub regions more easily. However, the transformation onto EUR-11 grid and to NetCDF format takes a lot of time and is not straight forward for those big data files, due to the high resolution and big domain. Which is why they have not yet been in use and the focus is on the smaller sub-domain.

Data-processing

For the purposes of exploring the potential of the CryoLand FSC dataset to be used as reference dataset for calibrating and bias-adjusting regional climate model (RCM) data the satellite data should be aggregated to the same resolution as the RCM data. Thus the CryoLand FSC data has to be re-gridded onto the CORDEX EUR-11 domain and grid, which has a horizontal resolution of $0.11^\circ \times 0.11^\circ$ on a rotated pole grid (corresponding to about $12.5 \text{ km} \times 12.5 \text{ km}$). Within this process the data is also transformed to the NetCDF format.

Experiences based on initial analyses

As climate data we used a simulation of RCA4 (SMHI regional climate model) on EUR-11, which was driven by a re-analysis product (ERA Interim, Dee et al. 2011). A re-analysis is a product assimilating different observations (station data, radio sondes, etc.) in combination with a forecast model to describe the recent history of earth's climate. It does not describe the day-to-day weather, but matches the current climate. By using re-analysis as driver for an RCM, the systematic bias of the RCM is revealed.

Simple time series of FSC for the study region have been produced. Here, the FSC from both datasets were summed up for the whole region and divided by the number of grid-cells with valid data to get the mean FSC for the whole study region. As a first comparison of the temporal evolution the difference between observation and climate model was calculated (Fig. 5.4). The first obvious thing is that RCA produces less snow than observed by the satellite. However, the major discrepancy is the existence of snow in summer in the observation. For that region there are no indications of snow cover during summer months. It is not generally impossible, but unlikely. However, it is impossible to observe snow cover every summer during the last 12 years. The underlying FSC-algorithm is rather sensitive to false cloud omissions; if a cloudy pixel is not recognized, it may be interpreted as snow, but this depends strongly on the local land cover, ground temperature and the also on the atmospheric conditions during the image acquisition. SYKE has recently developed a new methodology to avoid false snow caused by omitted clouds, but this method is not used in the current CryoLand dataset.

So the likely reason for falsely observed snow lies in the post-processing of the direct satellite data, i.e. when it gets converted to FSC. A cloud detection algorithm is applied which distinguishes between snow cover and cloud cover in the optical data. Even though this algorithm is sophisticated, it is not possible to capture every cloud event. In the case for CryoLand data this leads to too much snow in summer. For the other seasons, which are relevant for our studies, like the melt-off in spring or first snow in autumn, it is not clearly known if and how much snow is falsely reported. According to experience by SYKE (based on the cloud algorithm development work for the GlobSnow project), MODIS cloud mask strongly tends to generate false clouds over fractional snow, particularly over the snow line for example surrounding the mountains. As a consequence only high snow fractions or full snow cover will retain, while low snow fractions are labelled as 'clouds'. This leads to overestimation on FSC when converting the original FSC's into the CORDEX EUR-11. This is very likely one reason for differences reported in this section.

It can be assumed that this issue is less present in regions with all year snow cover. Those regions lie far north but are shadowed during parts of the year (winter) from the satellite. However, in the further progress of this study one could consider a study region in northern Scandinavia as the "data loss" due to shadowing is less or about the same as snow less months in summer in other regions.

One potential approach for now is to cut out summer months and not include them in the analysis. Another option would be to use a static mask of FSC=0% for such regions (time dependently) where snow is practically an impossible event, statistically spoken. This kind of approach is practiced e.g. in the NASA MODIS V005 snow products, where e.g. the most southern parts (and deserts etc.) are always

labelled snow-free. CryoLand does not apply this kind of masking, but it is of course possible to post-process the data like this. However, for the other seasons there is no clear solution in the short run. Thus, a possibility would be to continue with the planned analysis assuming/defining the satellite snow observations as reality, but mentioning clearly they actually are not correct. As the aim is to establish to what extent the CryoLand FSC data can be used as reference dataset for bias-correction of RCM data, this is not a viable approach. To meet this aim it is essential that the reference data set do not add another source of unaccounted bias into the corrected dataset.

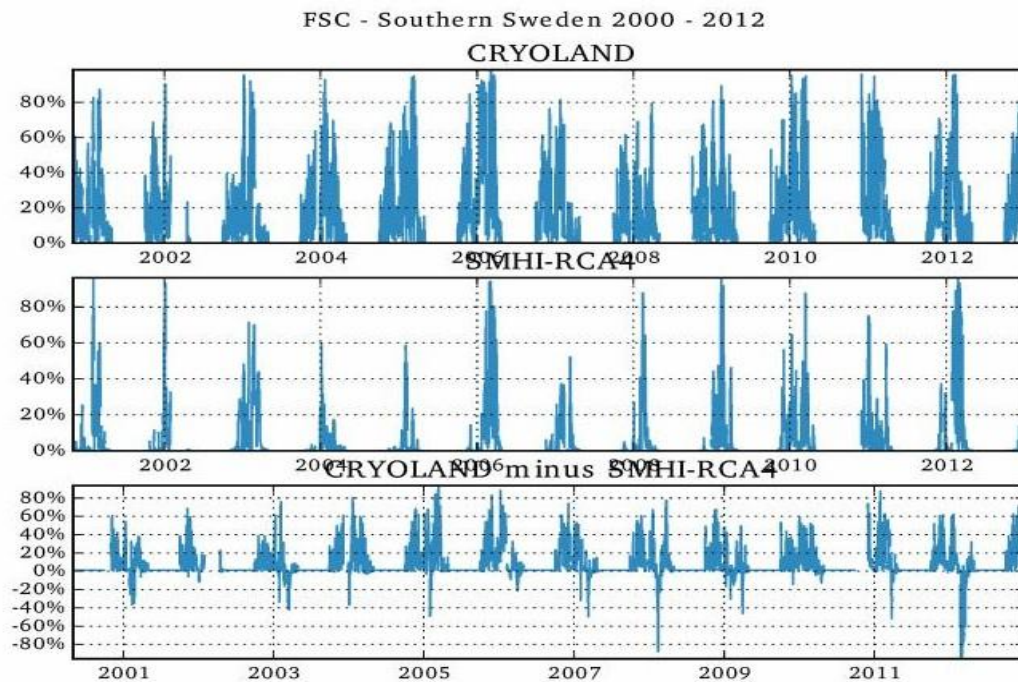


Figure 5.4: FSC time series of observation (upper panel), RCA-ERAInterim (middle panel), and difference of the two (lower panel) summed over the study region.

For the future

A better way, but more time-consuming, would be to re-do some steps. With the CryoLand FSC data an uncertainty estimate data set is provided. Specifically, for each grid cell on each day an uncertainty value is assigned to the data value. Using these uncertainty data on the 500m × 500m resolution and setting all data values (every single day and grid cell) with high uncertainty (above some threshold) to “Not Available” could result in a “cleaner” reference data set. Then all the processing (aggregation and re-gridding) would have to be repeated and an analysis could be tried again. However, as stated in Section 2.1.3, the current uncertainty layer included only non-biased RMSE (i.e. systematic error component is missing), which complicates its use as the current form. In addition, the current uncertainty estimates is likely a bit too ‘pessimistic’ estimate for uncertainty for forested areas. Hence, using a threshold for ignoring very uncertain areas would lead to exclusion of dense forest particularly. So SYKE suggest that so far ‘cleaning’ the dataset like suggested above is not the best way to go. Furthermore, according to the evaluation work carried out in ESA SnowPEX project (not published yet), CryoLand performs about equally well as NASA MODIS snow product in discriminating between ‘snow’ and ‘non-snow’, either using FSC=15% or FSC=50% when converting FSC information to these two classes. This is the case for the dominating snow classes ‘Ephemeral snow’, ‘Maritime snow’ and ‘Mountain snow’ (Sturm et al., 1995). Particularly for ‘maritime snow’ which is dominant in Europe, CryoLand seems to perform best throughout the year, and it also gives the highest scores in the snow accumulation period for all snow types i.e. throughout Europe. For these reasons, the above suggested mechanical approach of ignoring the most uncertain FSC estimates is not recommended; instead SYKE suggests that this could

be done according to land cover, Sturm snow classification and temporal season. However this approach would require further investigation and perhaps is not possible within CLIPC with the current resources.

Further analysis which is considered would cover the maximal snow extend (area), the variability of the snow extent, and the annual cycle of snow extent.

In any case it would be good to explore the possibility to use more than one observational data set for the analysis. Using multiple observational data sets when possible or available is important for the assessment of uncertainty, even if it only a part of the spread which would be covered. This is shown recently by Sunyer et al. (2013) for precipitation and holds even truer for variables, which are more difficult to observe like snow. A second observation source would increase the quality of the analysis and the validation of RCMs. However, a prerequisite is of course that the remote sensing datasets are compatible in terms of their geophysical information content. For Europe, there are only very few EO-product time series providing FSC. Most of the products provide only binary snow/non-snow information. The FSC-products have been evaluated under e.g. ESA project SnowPEX (still in progress), and the conclusion so far is that CryoLand and NASA MODIS snow products provide the highest – almost equal – accuracy. Basically it is possible to test also MODIS snow products, but the problem with clouds would not be solved as they use the exactly same cloud mask. EUMETSAT H-SAF products H12 (in pre-operational phase) may be also available, but due to the problems with AVHRR geolocation, the quality is poorer than that of CryoLand and NASA MODIS. H-SAF H12 relies on the same algorithm SCAMod) as CryoLand, applied to AVHRR data. Due to the above listed reasons, SYKE recommends to test SYKE's own FSC time series generated under Monimet project (<http://monimet.fmi.fi/index.php?style=warm&page=Project>). This dataset is also based on MODIS satellite observations and the retrieval algorithm for FSC is the same as for the CryoLand project (SCAMod), but cloud masking is done with an algorithm by SYKE, which so far has been found to work better for fractional snow/cloud discrimination than that used in CryoLand. Its spatial coverage is not as extensive as that of CryoLand, but it covers the Baltic Sea drainage basin and the surroundings and would thus be very useful for repeating the tests for Sweden to get insight on the impact of cloud mask into the FSC retrievals.

Finally, we note that some of the problems we have encountered in this work are of purely practical and technical nature. For example, different data formats, and name conventions and approaches for dealing with meta-data, as well as the limitations in data server capacity and the design choices required optimising the use of limited technical infrastructure for handling a huge dataset. These problems are all possible to handle and overcome, and one side effect of the work is of course to gain experience as well as highlight such bottlenecks so that they can be teased out in the future. However, other difficulties are of more profound nature and pertain more to the fundamentally different contexts for producing climate datasets and remote sensing (Earth observation) datasets.

With satellite data time series always being too short for climate research, they now reach time series of about 15 to 20 years length, which we acknowledge as a long time series from a remote sensing perspective. Together with the high resolution (1 km or below), satellite data shifts now into the view of climate research. However, there are still some caveats which need more attention before this data can be used widely within the climate field. Climatologies are usually defined with at least 30 years of continuous data to account for, e.g., decadal variability in the climate system. This is not only relevant for analysing climate models, but also for calibration of bias correction methods. 20 years of observation may not be sufficient for most of the studies. In essence, the required averaging period depends on the inter-annual variability of the analysed phenomenon.

It is also acknowledged that the provision of complete time series by satellite products is of enormous value. However, in climate science the time series need not only be “complete” in temporal sense, but also in spatial. It is understandable that satellite data provide slightly “patchy” time series as satellites pass the earth in paths at a time. It is, however, important for climate analysis when the observation took place, and that it is homogeneous with the neighbouring observations.

In contrast to that is the very high resolution of 500 m, in this case. This resolution seems very valuable for climate impact science, which often relates to the same or even higher resolved problems. In the field of climate modelling high resolution is still around 10 km and only very slowly moving towards 6 km or 2-3 km.

6 Summary and conclusions

A number of satellite based datasets for climate change indicator indices were acquired and assessed and results presented in this document. There are several promising candidates among, e.g. the ESA CCI programme, ESA GlobSnow and EC CryoLand that were documented and also examined for application for bias correction of climate model data.

A number of climate change indicators were derived from the satellite data and a selected number of the most relevant ones were presented in this document.

As an example and precursor to future similar studies an assessment of climate model data, in comparison with satellite-derived GlobSnow SWE data was presented and preliminary work on bias correction, using CryoLand FSC data was described.

The work carried out is a fair start for a field that has not been thoroughly investigated so far. Several problems and issues in the data and approaches suitable for the work were identified and early progress shows that there is potential to utilize the unique satellite-based datasets for both bias correction of climate model data and an independent “ground truth” reference data.

Further investigations are still underway and will be presented and discussed in CLIPC final report.

A publication of the research efforts presented in this deliverable and the lessons learned is currently under preparation.

References

- Bicheron, P., Defourny, P., Brockmann, C., Schouten, L., Vancutsem, C., Huc, M., Bontemps, S., Leroy, M., Achard, F., Herold, M., Ranera, F. & Arino, O. (2008). GLOBCOVER Products Description and Validation Report. Medias France, Toulouse, France. Available at: http://due.esrin.esa.int/globcover/LandCover_V2.2/GLOBCOVER_Products_Description_Validation_Report_I2.1.pdf
- Brodzik, M. J. and K. W. Knowles. 2002. EASE-Grid: A Versatile Set of Equal-Area Projections and Grids in M. Goodchild (Ed.) Discrete Global Grids. Santa Barbara, California USA: National Center for Geographic Information & Analysis.
- Bärring, L., T. Landelius, R.A.I. Wilcke, P. Dahlgren, G. Nikulin, S. Villaume, P. Undén, P. Kållberg, 2014: A new high-resolution European region reanalysis dataset for RCM evaluation and calibration – first tests and comparison to other datasets. RCM2014 Workshop Proceedings, 3rd International Lund RCM Workshop: 21st Century Challenges in Regional-scale Climate Modelling, Lund, Sweden, 16-19 June 2014. International Baltic Earth Secretariat Publication, No 3, 387 pp.
- Christensen, J.H., Boberg, F., Christensen, O.B., Lucas-Picher, P. (2008). On the need for bias correction of regional climate change projections of temperature and precipitation. *Geophys. Res. Lett.* 35 (20), L20709, <http://dx.doi.org/10.1029/2008GL035694>.
- Costa, Luís, Mikael Hildén, Jürgen Kropp, Kristin Böttcher, Stefan Fronzek, Rob Swart, Julianne Otto, Niall McCormick, Milka Radojevic, Johannes Lückenköter, Elke Keup-Thiel, Kari Luojus, Anni Törhönen, Jenni Attila, Heidi Pirtonen, Tanya Singh, Olli-Pekka Mattila, Juha Pöyry, Emilia Sanchez, Jenni Attila, (2015). “A review of climate impact indicators across themes: Description of strengths, weaknesses, technical requirements and mismatches from user expectations” Deliverable of CLIPC project, available from http://www.clipc.eu/media/clipc/org/documents/deliverables/clipc_del7%201_final.pdf
- Dee, D. P., Uppala, S. M., Simmons, A. J., Berrisford, P., Poli, P., Kobayashi, S., Andrae, U., Balmaseda, M. A., Balsamo, G., Bauer, P., Bechtold, P., Beljaars, A. C. M., van de Berg, L., Bidlot, J., Bormann, N., Delsol, C., Dragani, R., Fuentes, M., Geer, A. J., Haimberger, L., Healy, S. B., Hersbach, H., Hólm, E. V., Isaksen, I., Kållberg, P., Köhler, M., Matricardi, M., McNally, A. P., Monge-Sanz, B. M., Morcrette, J.-J., Park, B.-K., Peubey, C., de Rosnay, P., Tavolato, C., Thépaut, J.-N. and Vitart, F. (2011), The ERA-Interim reanalysis: configuration and performance of the data assimilation system. *Q.J.R. Meteorol. Soc.*, 137: 553–597. doi:10.1002/qj.828
- Doran, G.T., (1981). There's a S.M.A.R.T. way to write management's goals and objectives. *Management Review*, 70(11), 35-36.
- Elsasser H., Burki R., 2002: Climate change as a threat to tourism in the Alps. *Climate Research*, 20(3), 253-257. DOI: 10.3354/cr020253
- GCOS-195 (2015), “Status of the Global Observing System for Climate”, World Meteorological Organisation, available from: http://www.wmo.int/pages/prog/gcos/Publications/GCOS-195_en_LowRes.pdf
- Haylock, M.R., N. Hofstra, A.M.G. Klein Tank, E.J. Klok, P.D. Jones, M. New. 2008: A European daily high-resolution gridded dataset of surface temperature and precipitation. *J. Geophys. Res (Atmospheres)*, 113, D20119, doi:10.1029/2008JD10201
- Klein Tank, A.M.G., F.W. Zwiers and X. Zhang, 2009. Guidelines on Analysis of extremes in a changing climate in support of informed decisions for adaptation. WMO-TD No. 1500, 56 pp.
- Lemmetyinen, J., C. Derksen, J. Pulliainen, W. Strapp, P. Toose, A. Walker, S. Tauriainen, J. Pihlflyckt, J.-P. Kärnä, and M. T. Hallikainen., (2009) "A comparison of airborne microwave brightness temperatures and snowpack properties across the boreal forests of Finland and western Canada." *IEEE Transactions on Geoscience and Remote Sensing*, 47: 965–978.
- McCormick, N. and N. Gobron. 2015. Assessment and Monitoring of Negative Impacts of Climate Change on Land Vegetation in Developing Countries, using Earth Observation (EO) Satellite Data. Draft Technical Report,

European Commission (EC), Joint Research Centre (DG JRC), Institute for Environment and Sustainability (IES).
Draft version: 31 July 2015.

Melia, N., K. Haines, and E. Hawkins, (2015), "Improved Arctic sea ice thickness projections using bias-corrected CMIP5 simulations" 9, 2237-2251, doi:10.5194/tc-9-2237-2015.

Merchant, C.J.; Embury, O.; Roberts-Jones, J.; Fiedler, E.K.; Bulgin, C.E.; Corlett, G.K.; Good, S.; McLaren, A.; Rayner, N.A.; Donlon, C. (2014): ESA Sea Surface Temperature Climate Change Initiative (ESA SST CCD): Analysis long term product version 1.0. NERC Earth Observation Data Centre, 24 February 2014. doi: 10.5285/878bef44-d32a-40cd-a02d-49b6286f0ea4.

Metsämäki, S., Anttila, S., Huttunen, M., Vepsäläinen, J. (2005). A feasible method for fractional snow cover mapping in boreal zone based on a reflectance model. *Remote Sensing of Environment*, 95, 77–95.

Metsämäki, S., Mattila, O.-P., Pulliainen, J., Niemi, K., Luojus, K. & Böttcher, K. (2012). An optical reflectance model-based method for fractional snow cover mapping applicable to continental scale. *Remote Sensing of Environment*, 123, 508–521.

Metsämäki, S., Pulliainen, J., Salminen, M., Luojus, K., Wiesmann, A., Solberg, R., Böttcher, K., Hiltunen, M., Ripper, E. (2015). Introduction to GlobSnow SE-products with considerations for accuracy assessment. *Remote Sensing of Environment*, 156 (2015) 96–108.

Nagler, T. Bippus, G., Schiller, C., Metsämäki, S., Mattila, O.-P., Luojus, K., Malnes, E., Solberg, R., Diamandi, A., Larsen, H.E., Wiesmann, A., Gustafsson, D. (2015): CryoLand - Copernicus Service Snow and Land Ice: Final Report, pp. 46. available at <http://cryoland.eu> and <http://enveo.at>.

Ovaskainen O., Skorokhodova S., Yakovleva M., Sukhov A., Kutenkov A., Kutenkova N., Shcherbakov A., Meyke E., Delgado M.D., 2013: Community-level phenological response to climate change. *Proc. Nat., Acad. Sci.*, 110(33), 13434-13439. DOI: 10.1073/pnas.1305533110

Pulliainen, J., J. Grandell, and M. T. Hallikainen. (1999) HUT Snow Emission Model and its Applicability to Snow Water Equivalent Retrieval. *IEEE Transactions on Geoscience and Remote Sensing*. 37: 1378-1390.

Pulliainen, J., (2006) Mapping of snow water equivalent and snow depth in boreal and sub-arctic zones by assimilating space-borne microwave radiometer data and ground-based observations. *Remote Sensing of Environment*. 101: 257-269. DOI: 10.1016/j.rse.2006.01.002.

Seneviratne, S. I., et al., (2012). Changes in climate extremes and their impacts on the natural physical environment, in *Managing the Risks of Extreme Events and Disasters to Advance Climate Change Adaptation: A Special Report of Working Groups I and II of the Intergovernmental Panel on Climate Change (IPCC)*, edited by C. B. Field et al., pp. 109–230, Cambridge Univ. Press, Cambridge, U. K.

Sunyer, M. A., Sørup, H. J. D., Christensen, O. B., Madsen, H., Rosbjerg, D., Mikkelsen, P. S., and Arnbjerg-Nielsen, K.: On the importance of observational data properties when assessing regional climate model performance of extreme precipitation, *Hydrol. Earth Syst. Sci.*, 17, 4323–4337, doi:10.5194/hess-17-4323-2013, 2013.

Takala, O. M., Pulliainen, J., Metsämäki, S., & Koskinen, J. (2009). Detection of snowmelt using spaceborne microwave radiometer data in Eurasia from 1979 to 2007. *IEEE Transactions on Geoscience and Remote Sensing*, 47, 2996–3007.

Takala, M., Luojus, K., Pulliainen, J., Derksen, C., Lemmetyinen, J., Kärnä, J.-P., Koskinen, J. and Bojkov, B., (2011). Estimating northern hemisphere snow water equivalent for climate research through assimilation of space-borne radiometer data and ground-based measurements, *Remote Sensing of Environment*, Vol. 115, 12: 3517-3529. doi: 10.1016/j.rse.2011.08.014

van den Besselaar, E.J.M., M.R. Haylock, G. van der Schrier and A.M.G. Klein Tank. 2011: A European Daily High-resolution Observational Gridded Data set of Sea Level Pressure. *J. Geophys. Res.*, 116, D11110, doi:10.1029/2010JD015468

Wilcke Renate, Barring Lars, Dobler Andreas, Nikulin Grigory, Vautard Robert, Vrac Mathieu, Braconnot Pascale, Otto Juliane, Haugen Jan Erik (2015). CLIPC Deliverable 6.1: Climate model data for Europe

Zhang, X., G. Hegerl, F. W. Zwiers, J. Kenyon (2005), Avoiding Inhomogeneity in Percentile-Based Indices of Temperature Extremes. *J. Climate*, 18, 1641-1651, doi:<http://dx.doi.org/10.1175/JCLI3366.1>